General Disclaimer

One or more of the Following Statements may affect this Document

- This document has been reproduced from the best copy furnished by the organizational source. It is being released in the interest of making available as much information as possible.

- This document may contain data, which exceeds the sheet parameters. It was furnished in this condition by the organizational source and is the best copy available.

- This document may contain tone-on-tone or color graphs, charts and/or pictures, which have been reproduced in black and white.

- This document is paginated as submitted by the original source.

- Portions of this document are not fully legible due to the historical nature of some of the material. However, it is the best reproduction available from the original submission.

NASA TECHNICAL MEMORANDUM NASA TM-75548

OPTICAL CHARACTERISTICS OF THE EARTH'S SURFACE AND ATMOSPHERE FROM THE POINT OF VIEW OF THE REMOTE SENSING OF NATURAL RESOURCES (REVIEW OF THE CONTEMPORARY STATUS OF THE PROBLEM)

V. I. Tarnopol'skiy

Translation of "Opticheskiye Kharakteristiki Poverkhnosti i Atmosfery Zemli s Tochki Zreniya Distantsionnogo Issledovaniya Prirodnykh Resursov," Academy of Sciences USSR, Institute of Space Research, Moscow, Report PR-287, 1976, 73 pages

NATIONAL AERONAUTICS AND SPACE ADMINISTRATION
WASHINGTON, D.C. 20546 OCTOBER 1978

STANDARD TITLE PAGE

1. Report No. NASA TM-75548	2. Government Accession No.	3. Recipient's Catalog No.
4. Title and Subtitle OPTICAL CHARACTERISTICS OF THE EARTH'S SURFACE AND ATMOSPHERE FROM THE POINT OF VIEW OF REMOTE SENSING OF NATURAL RESOURCES		5. Report Date October 1978 6. Performing Organization Code
7. Author(s) V. I. Tarnopol'skiy USSR Academy of Sciences Institute of Space Research		8. Performing Organization Report No. 10. Work Unit No.
9. Performing Organization Name and Address Leo Kanner Associates Redwood City, California 94063		11. Contract or Grant No. NASW-3199 13. Type of Report and Period Covered Translation
12. Sponsoring Agency Name and Address National Aeronautics and Space Administration, Washington, D.C. 20546		14. Sponsoring Agency Code

15. Supplementary Notes

Translation of "Opticheskiye Kharakteristiki Poverkhnosti i Atmosfery Zemli s Tochki Zreniya Distantsionnogo Issledovaniya Prirodnykh Resursov," Academy of Sciences USSR, Institute of Space Research, Moscow, Report PR-287, 1976, 73 pages

16. Abstract Widely used remote probing methods, and especially the multi-spectral method, for studying the earth from aerospace platforms necessitate the systematization and accumulation of data on the relationships between remote observations and measured parameters and characteristic properties and conditions of phenomena on the earth's surface.

Herein we present and systematize data on the optical characteristics of natural objects which arise during observations of these objects over a wide spectral interval which encompasses solar radiation reflected by the object as well as the object's inherent thermal radiation. We discuss the influence of the earth's atmosphere on remote measurements and several problems in simulation and calculation.

17. Key Words (Selected by Author(s))	18. Distribution Statement
	Unclassified-Unlimited

19. Security Classif. (of this report)	20. Security Classif. (of this page)	21. No. of Pages	22. Price
Unclassified	Unclassified		

NASA-HQ

PREFACE

Remote sensing of the earth's surface from distant aerospace platforms eventually results in the recognition of concrete objects and determinations of their conditions by relating them to a category of objects with fixed conditions. This classification is based on results of measurements of one of several physical values which are related to the properties and condition of the object and which are signs by which the object is recognized. Using a multi-spectral method in the optical range of electromagnetic radiation by these signs, it is possible to measure the spectral brilliances of concrete objects with the probing system. Thus, to construct an adequate model of the process of remote sensing and of the system of gathering and processing data, it is necessary to establish a connection between the type and condition of terrestrial formations and the measured spectral brilliance values. This is impossible without a prior analysis of the properties and described characteristics of the natural components which are involved in remote sensing.

At first we determine the spectral regions for which this analysis is necessary. It is well known that the sun is the most powerful emitter in our planetary system. The sun creates irradiance with spectral distribution of values $E_0(\lambda)$, shown in Fig. 1, on the upper layer of the earth's atmosphere. In addition to the sun, irradiators external to terrestrial objects include the moon, the planets, and the stars. However, the radiation produced by these celestial bodies is quite insignificant in comparison to that produced by the sun (Fig. 2) so that in the future we will refer only to the sun as the external irradiator which affects the earth.

The terrestrial objects which we use as objects in remote sensing obviously have temperatures higher than absolute zero and thus, their inherent thermal radiation may be observed[1]. However, since the majority of terrestrial objects have temperatures which are significantly lower than the temperature of the sun's outer envelope ($\approx 6000^\circ$ K), in accordance with thermal radiation principles [2], the maximum spectral distribution of radiation densities are observed in longer wave intervals than those of the sun (Fig. 3). Practically, for wavelengths $\lambda < 3.5$ μm, the inherent radiation of natural objects is negligible in comparison to reflected solar radiation [19]. In probing in regions where $\lambda > 3.5$ m, the intensity of the inherent radiation of the objects studied exceeds reflected solar radiation [12].

1. Obviously, the thermal radiation of natural objects is also caused by the energy of the sun.

Thus, surveying the characteristics of an external irradiator (the primary radiation source) and the inherent radiation of the objects under study (secondary radiation sources) allows us to separate two spectral regions for remote probing- reflected ($\lambda < 3.5\ \mu m$) and inherent ($\lambda > 3.5\ \mu m$) radiation, and to examine further the basic relation between the properties of investigated objects and signals received by the multi-spectral optical scanning system. This is done for each of the separate spectral regions without disturbing the physical integrity of the remote sensing picture.

TABLE OF CONTENTS

OPTICAL CHARACTERISTICS OF THE EARTH'S SURFACE AND ATMOSPHERE FROM THE POINT OF VIEW OF THE REMOTE SENSING OF NATURAL RESOURCES (REVIEW OF THE CONTEMPORARY STATUS OF THE PROBLEM)

V. I. Tarnopol'skiy
USSR Academy of Sciences, Institute of Space Research

1. Spatial-Brilliance Characteristics of Terrestrial Formations

/5*

The chance arrangement of various objects within the limits of the survey system which collects video information results in the random structure in the brilliance field which we studied. Due to continuous changes in atmospheric conditions and in irradiation of the landscape, the brilliance of each element in a given object is also irregular at each moment in time in direction (Θ, Φ), i.e.

$$B(\lambda, \Theta, \varphi) = \xi(x, y, t), \quad (1)$$

where ξ is the random function of the X and Y coordinates of the given underlying surface region and time is t. In addition to this, the brilliance observed in the elementary region of the earth's surface depends on the extent of shading or illumination of neighboring regions on the surface, i.e. it is related to the relief characteristics of the site and to the relative orientations of the sun and the probing system. The above information allows us to consider any formation studied as a random brilliance field.

The random brilliance field, which is the subject of our study, suitably describes characteristics such as the distribution of brilliance probabilities $p(B)$ and spatial frequencies $P(\Omega)$, the correlation function $K(\ell)$ and the spectral density of the spatial brilliance distribution in subject $Q(\Omega)$ [1, 20].

/6

We turn first to the examples presented in [20] of the logarithmic laws of brilliance distribution $P(\ell g\ B)$ for various groups of natural objects, as illustrated in Fig. 4. Evidently, the basic differences in the characteristics of these groups of objects show up in the average values and dispersions of the brilliance logarithms. We also note that this distribution is intermediate between uniform and standard but that it gravitates towards the latter. Because of this, the most suitable description of the variation in brilliance is obtained by using a logarithmic scale of measurement. Moreover, a logarithmic description is usually preferable for describing absolute variations in spectral brilliance because variations in absolute brilliance are often not comparable in the spectral intervals studied [30]. Measurements in narrow spectral intervals of the brilliance field of

* Numbers in the margin indicate pagination in the foreign text.

relatively homogeneous objects, which as a whole are associated with one of the selected categories of the representative alphabet often approximate the distribution of inherent brilliance by the normal law [9, 31]. This allows us to simplify the identification model at the first step.

The distribution of frequency describes the structure of the brilliance field and is its second characteristic [1]. The principle of this distribution $P(\Omega)$ is determined by the average frequency $\bar{\Omega}$ and dispersion frequency $\delta^2(\Omega)$, which conform to the average geometric size of the homogeneous objects and to the geometric homogeneity of the subject as a whole. Due to the limitless variation in natural landscapes, the principles of the distribution of geometric elements may also be variable. However, it was confirmed in [1] that they must all be related to assymetric distribution. A possible explanation of this is that the major components of the subject are composed of smaller ones, and that therefore, the probability of the small components will always exceed that of the larger ones. /2

The correlation function $K(\ell)$ is related to the Fourier transformation

$$\left.\begin{aligned} K(\ell) &= \frac{1}{\pi}\int_0^\infty Q(\Omega)\cos\Omega\ell\, d\ell \\ Q(\Omega) &= 2\int_0^\infty K(\ell)\cos\Omega\ell\, d\Omega \end{aligned}\right\} \quad (2)$$

the spectral density $Q(\Omega)$ clearly describes the frequency-contrast structure of the brilliance field, which characterizes the extent of the relation between the brilliance values for different parts of the subject and the distribution of brilliance according to spatial frequencies. This agrees closely with existing methods for evaluating the quality of surveying systems. In Fig. 5,...10 examples of the series of terrestrial formations described are shown. The data was obtained by telephotometric tracking from a low-flying airplane [20]. It is interesting that in the majority of examples of maximum spectral density, the dominant frequencies are characterized by hidden periodicity within the interval of spatial frequencies $0.05 \div 0.1\ m^{-1}$. This emphasizes, perhaps, some inherent necessity for a spatial clearance in surveying systems.

2. Spectral-Brilliance Characteristics of Terrestrial Formations

We further examine the nature and structure of characteristics of the spectral brilliance of terrestrial formations while considering the basis provided above for selecting two characteristic spectral regions from the optical range of electromagnetic variations.

The Range of Reflected Radiation. From observations in this range of the spectrum we see that the brilliance of the majority of natural objects and phenomena is dependent on their abilities to reflect and disperse electromagnetic radiation which falls on them[1]. In this case, the value of the spectral brilliance of the object is a function of the intensity of incident rays and the reflective properties of the object, i.e. /8

$$B_0(\lambda, \theta, \varphi) = f_1\{E_0(\lambda)\}, \quad (3)$$

where $B_0(\lambda, \theta, \phi)$ is the brilliance of the object in direction (θ, ϕ) and $E_0(\lambda)$ is the total illumination of the object.

It is customary to use the spectral brilliance coefficient to detect the functional dependence (3). According to [9, 15] the brilliance coefficient of a surface $r(\lambda, \theta, \phi)$ in the wavelength interval $(\lambda, \lambda + d\lambda)$ in the given direction (θ, ϕ) and under the given illumination conditions, the relation of the brilliance in the direction $B(\lambda, \theta, \phi)$ to orthotropic brilliance $B^L(\lambda)$ of a fully reflective surface, is found in these irradiation conditions, i.e.

$$r(\lambda, \theta, \varphi) = \frac{B(\lambda, \theta, \varphi)}{B^L(\lambda)}. \quad (4)$$

For this expression (3) will take the form

$$B_0(\lambda, \theta, \varphi) = B^L(\lambda) \cdot r(\lambda, \theta, \varphi) = \frac{1}{\pi} E_0(\lambda) r(\lambda, \theta, \varphi). \quad (5)$$

Inasmuch as the sun, in the first approximation, appears to be a fairly stable irradiator[2], under fixed measurement conditions /9

---

1. In a series of specific instances [23], the brilliance of natural objects fully or completely depends on the appearance of fluorescein, luminescein, etc, which were not considered in this work.

2. The normal density of the integral flow of solar radiation E_0 in the upper layer of the atmosphere varies systematically with the change in the distance between the sun and the earth: in January E_0 is 3.4% greater, and in July 3.4% less than the average annual values. Furthermore, there is some variation in the values for E_0 depending on the activity of the sun (this change is mostly

(among them $E_0(\lambda)$), measurements on the value of the measured brilliance $B(\lambda, \theta, \phi)$ will depend on the change $\Gamma(\lambda, \theta, \phi)$ of objects which fall within the system's instantaneous field of vision, i.e. the differences among objects or the condition of a single object will be based on evaluations of $\Gamma(\lambda, \theta, \phi)$.

Aside from spectral brilliance coefficients, integral brilliance coefficients and spectral and integral albedo values are used to describe the reflective properties of natural formations [9].

The integral brilliance coefficient is determined by the relation

$$\Gamma(\theta, \varphi) = \frac{\int_0^\infty B(\lambda, \theta, \varphi)\, d\lambda}{\int_0^\infty B^*(\lambda)\, d\lambda}. \qquad (6)$$

Spectral albedo $A(\lambda)$ is the value of the ratio of the stream of rays $F_\uparrow(\lambda)$, reflected by the object, to the rays falling on this object $F_\downarrow(\lambda)$, for some wave length interval $(\lambda, \lambda + d\lambda)$:

$$A(\lambda) = \frac{F^*(\lambda)}{F^*(\lambda)}. \qquad (7)$$

The integral albedo A is determined by an analogous method (6), and is namely: /10

$$A = \frac{\int_0^\infty F^*(\lambda)\, d\lambda}{\int_0^\infty F^*(\lambda)\, d\lambda} = \frac{\int_0^\infty A(\lambda) \cdot F^*(\lambda)\, d\lambda}{\int_0^\infty F^*(\lambda)\, d\lambda}. \qquad (8)$$

In general there is a clear connection between albedo and the brilliance coefficient [19]

$$A = \int_0^{\pi/2} \int_0^{2\pi} \Gamma(\theta, \varphi) \cdot \cos\varphi \cdot \sin\varphi\, d\varphi\, d\theta. \qquad (9)$$

It is not difficult to see that the numerical values for the albedo and the brilliance coefficient are the same for objects with orthotropic reflection.

As will be shown below, the value of the brilliance coefficient may vary not only with changes in the sighting direction, (θ, ϕ) but also with changes in the direction of the stream of incident rays. Therefore, a bidirectional (spectral) brilliance coefficient $\Gamma(\theta_1, \theta_2, \phi_1, \phi_2)$ is sometimes used. In the present case, where the irradiator is the sun, the bidirectional brilliance coefficient takes the form $\Gamma(Z_0, \theta, \phi)$.

---

related to the sun's short wave radiation) 5.

The reflective properties of terrestrial objects and formations have already been studied for a long time (several decades), however, a significant amount of the accumulated material is contradictory and poorly suited to accurate comparisons and statistical analysis. This situation results from essential discrepancies in the methods of measurement and in the capabilities of the instruments used by different authors. In addition to these factors, most of the investigations conducted have dealt only with the range 0.4÷0.9 μm; there is significantly less published data on the range 0.9÷3 μm.

However, the range of spectral brilliance coefficients and spectral albedo for some terrestrial formations which are relatively frequently observed, shown in Fig. 11-16, demonstrates, /11
without a strict analysis, the significant differences between their reflective properties. The possibility of systematizing similar data [15][3] shows that the differences in reflecting properties are not random but conform to defined regularities (Fig. 17).

It is clear that significant and persistent differences in spectral reflective properties exist not only among inherently different terrestrial formations, but are also determined by the conditions of the given formation. Inasmuch as the possibility of determining not only the class of an object but also its conditions is one of the key conditions of remote observations, we illustrate with several examples.

The essential factor on which the spectral reflective properties of plants mainly depend is their stage of vegetation [9]. In immature flora there is a characteristic bright green color at sufficiently high values of $r(\lambda)$. With the progression of the seasons, the leaves become saturated with chlorophyll and "darken", especially in the infrared region (Fig. 18). The change to autumnal coloring- yellowing - results in a disappearance of the chlorophyll absorption bands and an increase in the reflective capability in the visible range of the spectrum. Complete dessication results in $r(\lambda)$ values similar to those for light-colored soil (Fig. 19,...21). Changes in the reflective properties of plants are clearly related to changes in leaf surface conditions /12
such as those caused by pests etc. (Fig. 22). Another factor which results in changes in the behavior of $r(\lambda)$ for plants, including seasonal changes, is the variation in the water content of

---

3. One of the first and currently most widely used classifications of the spectral reflective properties of terrestrial formations is that proposed by E. L. Krinov in 1947. These classifications resulted from comparisons of diverse spectral measurements which he made using the photographic method (0.4÷0.9 μm)

the leaves (Fig. 23).

The spectral reflective capability of soil depends on the condition of its surface and is strongly correlated with its components, including organic substances (Fig. 24). The spectral brilliance coefficient of sand is also correlated to a significant degree with its petrographic composition (Fig. 25). In particular, the reflective capability of sand increases with an increase in the concentration of quartz grains and decreases with an increase in the concentration of heavy fractions, in this case the difference in $r(\lambda)$ values is more clearly expressed in the infrared section of the spectral region under consideration. As in the case of plants, the $r(\lambda)$ values for soil and sand are strongly dependent on their moisture contents (Fig. 26,27).

The degree of turbidity may have an effect on the spectral reflective capability of water (Fig. 28). Also important are the concentration of various dissolved and undissolved additives [9], chlorophyll (Fig. 29a) and plankton [23], petroleum contamination of the surface (Fig. 29b) etc. "Age", the condition of the surface, and the presence of contaminants are important to the spectral reflectivity of snow and ice. (Fig. 16).

The remotely measured value of $r_{(\lambda)}$ (more precisely $B_{(\lambda,\theta,\phi}$) is also influenced by the fine-structure spatial organization of the object under study [16]. Examples of the influence of this factor may include the change in $r(\lambda)$ for different projected floral coverings on soil (Fig. 30). Evidently, with the known reflective spectrum of soil, the area of projective covering S_c may be evaluated, or, with known S_c, the type of plant may be determined. In turn, if the type of plant and S_c are known, the characteristics of the soil may be determined. The definite possibility also exists of establishing a connection between the brilliance coefficient of the soil-plant composition and the size of the floral mass and the optical characteristics of the soil, as illustrated in Fig. 31. /13

The Range of Inherent Radiation. The brilliance of natural formations in this spectral range depends to a greater degree than in the range of reflected radiation on composition and structure. Disregarding considerations of residual reflected radiation referred to above, we present this dependence in the form

$$B_0(\lambda, \theta, \varphi) = f_2\{R(\lambda)\}, \qquad (10)$$

where $R(\lambda)$ is the spectral distribution density of the radiation from the given object. The density of radiation of concrete substances, as is well known, is always less than the density of radiation of absolutely black substances at the same thermodynamic temperature T (see Fig. 3). As shown in [2], the ratio of the density of radiation $R(\lambda)$ of a concrete substance to that of

an absolutely black substance $R^{abs}(\lambda)$ in the wavelength interval $(\lambda, \lambda + d\lambda)$ is the spectral coefficient of radiation density $\varepsilon_R(\lambda)$, i.e.

$$\varepsilon_R(\lambda) = \frac{R(\lambda)}{R^{ABS}(\lambda)} , \qquad (11)$$

while, as is well known [2], the spectral distribution of values obeys Planck's law, namely:

$$R^{ABS}(\lambda) = 2\pi h c^2 \lambda^{-5} \left[\exp\left(\frac{ch}{\lambda k T}\right) - 1 \right]^{-1}, \qquad (12)$$

where h is Planck's constant, $6.6256 \cdot 10$ W /14

c is the speed of light, $2.9979 \cdot 10^8$ m.sec^{-1}; and

k is Boltzmann's constant, $1.38054 \cdot 10^{-23}$ W

Inasmuch as the spectral radiation density is related to spectral brilliance, the general relation

$$R(\lambda) = \int_0^{2\pi} \int_0^{\pi/2} B(\lambda, \theta, \varphi) \cdot \cos\varphi \cdot \sin\varphi \, d\varphi \, d\theta, \qquad (13)$$

and for an absolutely black substance which appears as an ideal Lambert irradiator [2]

$$R(\lambda) = \pi \cdot B(\lambda), \qquad (14)$$

relations (10) and (11) may lead to

$$B_o(\lambda, \theta, \varphi) = \frac{1}{\pi} R^{ABS}(\lambda) \cdot \varepsilon(\lambda, \theta, \varphi) \qquad (15)$$

and

$$\varepsilon_R(\lambda) = \int_0^{2\pi} \int_0^{\pi/2} \varepsilon(\lambda, \theta, \varphi) \cdot \cos\varphi \cdot \sin\varphi \, d\varphi \, d\theta, \qquad (16)$$

where $\varepsilon(\lambda, \theta, \phi)$ is the spectral radiation coefficient of the surface in the wavelength interval $(\lambda, \lambda + d\lambda)$, in a direction (θ, ϕ), equal to the ratio of the spectral brilliance in direction $B(\lambda\theta, \phi)$ to the spectral brilliance $B^{abs}(\lambda)$ of an absolutely black substance at the same temperature T, i.e.

$$\varepsilon(\lambda, \theta, \varphi) = \frac{B(\lambda, \theta, \varphi)}{B^{ABS}(\lambda)} . \qquad (17)$$

We note that the expression for $\varepsilon(\lambda, \theta, \phi)$ and the relation of $\varepsilon_R(\lambda)$ with $\varepsilon(\lambda, \theta, \phi)$ appears analogous to the ratio for the spectral brilliance coefficient (4) and for its relation with spectral albedo (9).

The value of the spectral radiation coefficient depends in the first place on the physical nature of the given object and on the condition of its surface (roughness, moisture, acidity, /15

etc.) and may vary with a change in the temperature of the object. Non-metals, which comprise the overwhelming majority of the terrestrial objects in which we are interested, have radiation coefficients which are usually close to one and which decrease insignificantly with a rise in temperature [2].

Investigations of the spectral radiation properties of natural formations were begun latter than investigations of reflective properties and are still in a less satisfactory condition. Most of the data on spectral radiation coefficient values at present relate to minerals [34, 35, 36, 38, 41, 43] and water [2]. Data on other natural objects is very scanty [12, 19]. In addition to the spectral radiation coefficient, $\varepsilon(\lambda)$ partial

$$\varepsilon_{\Delta\lambda} = \frac{\int_{\lambda_1}^{\lambda_2} \varepsilon(\lambda) \cdot R(\lambda)\, d\lambda}{\int_{\lambda_1}^{\lambda_2} R(\lambda)\, d\lambda}, \qquad (18)$$

and also total

$$\varepsilon = \frac{\int_{\lambda_1}^{\lambda_2} \varepsilon(\lambda) \cdot R(\lambda)\, d\lambda}{\int_{\lambda_1}^{\lambda_2} R(\lambda)\, d\lambda} \cdot \frac{1}{\sigma \cdot T^4} \int_0^{\infty} \varepsilon(\lambda) \cdot R(\lambda)\, d\lambda \qquad (19)$$

integral radiation coefficients are used to describe the radiative properties of non-black substances fairly frequently. In Fig. 32,...36 and in Table I are shown several examples of the spectral behavior of the values of $\varepsilon(\lambda)$ and $\varepsilon_{\Delta\lambda}$ and ε for a series of natural formations.

Despite the incompleteness of data on the spectral radiation capabilities of natural objects, especially in comparison with the various examples of their reflective properties, we may note the obvious dependence of values of $\varepsilon(\lambda)$ on chemical composition (in particular the SiO_2 composition), moisture, and roughness [36, 37]. Various types of natural formations have series of characteristic lines in the path of $\varepsilon(\lambda)$, however, the relative values of these differences are insignificant. /16

In contrast to remote measurements in the range of reflected radiation, where equation (5) may be solved for $\Gamma(\lambda, \theta, \phi)$ of a given object according to its measured brilliance for known irradiation conditions, in the range of inherent radiation this determination can not be done correctly, as in the general case the measured brilliance $B(\lambda, \theta, \phi)$ of any object in conformity with (12) and (15) is a function of its temperature T and radiation coefficient $\varepsilon(\lambda, \theta, \phi)$, which are unknown. Thus, as a result of the remote measurement of the inherent radiation brilliance $B(\lambda, \theta, \phi)$ of an object, its brilliance temperature $T_B(\lambda)$ appears, i.e. the equivalent temperature of a black substance, the brilliance of which, for a given spectral interval of measurement $(\lambda, \lambda + d\lambda)$, is equal to the obtained value for $B(\lambda, \theta, \phi)$ [2].

4. σ is the Stefan-Boltzmann constant, $5.6697 \cdot 10^{-16}$ W·m^2·deg.K^{-4} [24].

Evidently, for objects which have the same temperature T, differences in their brilliance temperatures $T_B(\lambda)$ may be determined by differences in their radiation coefficients $\varepsilon(\lambda)$.

According to (12), a difference in values of temperature T may have a significantly greater effect on results of measurements of $B(\lambda)$ or $T_B(\lambda)$ than differences in values of $\varepsilon(\lambda)$. For this reason we decide on several lines for a description of temperature conditions of terrestrial formations. In the first approximation we will consider, excluding geothermal phenomena and industrial activity which results in the release of thermal energy, that /17
the basic heat flow which acts on the radiating Lambert surface of an object is produced by the sun. The equation for the energy balance [24] for this case has the form:

$$\alpha S_0' \int_0^\infty E_0(\lambda)\, d\lambda = \varepsilon_R \cdot S_0 \cdot \sigma \cdot T^4 + P, \qquad (20)$$

where $\alpha = 1-A$ is the integral absorption coefficient of solar radiation on the surface of a given object;

S_0' is a projection of the radiating surface of an object onto a plane which is perpendicular to the direction of incident solar radiation;

S_0 is the value of the radiating surface of the object

P is a term in an equation which considers the effects of various heat transfer mechanisms in relation to the object.

Thus, the equilibrium temperature of the object under study is related to the integral albedo and the radiation coefficient of its surface. We note that absorption and emitting of radiation by the object occurs in essentially different spectral intervals. For example, during illumination of snow covers by the sun, the absorbed radiation is in the range of reflected radiation, and 98% of the radiation emitted by the snow is within the interval $3 \div 7\ \mu$m (the maximum, determined by the temperature of the snow is about $10.5\ \mu$m [24]. It is also interesting that, following from (15), with an increase in ε_R, the brilliance temperature T_B must also rise, and the equilibrium temperature T, according to (20), decreases. This evidently results in additional masking of the observed individuality of the objects. Nevertheless, temperature contrasts between the various natural objects reach perceptible /18
values [4, 38, 40].

From equation (20), the degree of irradiation of an object by the sun, as is well known, may change considerably and cause corresponding oscillations in the temperature of the object. The actual temperature curve, of course, may also be related to

the thermal inertia of the object, i.e. to its physical characteristics [43]. The daily changes in various types of road surfaces illustrated in Fig. 37 show, for example, that in comparison with a concrete surface, asphalt, which has better absorption capabilities and produces a finer surface, has a higher temperature and a greater amplitude in its daily cycle. The significant heat capacity of water, in turn, leads to a relatively smaller variation in the temperatures of water surfaces and damp soil coverings in the course of the diurnal cycle (Fig. 376). The surface temperature values at single moments in the diurnal cycle shown in Fig. 38 reveal their proportional relation to the degree of moisture present and to the density of the soil. The latter relation agrees with the dependence of thermal inertia on the density of various rock forming minerals, rocks, and soils (Fig. 39), as shown in [43]. Results show that at night, water and damp soil are warmer, and during the day cooler than dry soil. We considered the specifics of the diurnal temperature cycles of underlying surfaces in selecting observation times for specific investigations. In particular, for studies of geothermal zones or the mineral composition of outcrops, morning observations at the minimum point in the diurnal cycle are most suitable [37, 43].

3. The Relation between Properties of the Earth's Atmosphere and the Possibility of Doing Remote Sensing of the Underlying Surface

/19

The presence of a separating medium between the object under investigation and the information gathering system is a particular feature of remote probing methods. In the present case this medium is the earth's atmosphere, which is a mixture of gases and water vapor with small particles of various origins - aerosols - suspended in it [19]. At first we decide on the basic properties and described characteristics of the atmosphere which determine the regularities of the transfer of electromagnetic radiation currents of the optical range wavelength through it.

As is well known, a radiation current which is propagated in the atmosphere in a given direction (θ,ϕ) weakens. This is caused by the absorption of part of the radiation by molecules of atmospheric gases and aerosol and by scattering in heterogeneous densities in the air and in aerosol particles. The decrease in the monochromatic brilliance of the emitter observed in direction (θ,ϕ) across an atmospheric layer of thickness H is described by the Bouguer-Lambert law:

$$B(\lambda,\theta,\varphi) = B_0(\lambda,\theta,\varphi)\cdot\exp\left[-\int_{\Delta H}\alpha(\lambda)\,dH\right], \qquad (21)$$

where $\alpha(\lambda)$ is the weakening coefficient which depends in most cases on the wavelength λ and the concentration of absorbed and scattered components in a given segment of path ΔH, which is usually presented in the form [19]:

$$\alpha(\lambda) = \alpha_a(\lambda) + \alpha_s(\lambda). \qquad (22)$$

where $\alpha_a(\lambda)$ is the absorption coefficient and $\alpha_s(\lambda)$ is the scattering coefficient. The transmittance of an atmospheric layer of thickness ΔH is determined by

/20

$$T(\lambda,\theta,\varphi) = \frac{B(\lambda,\theta,\varphi)}{B_0(\lambda,\theta,\varphi)} = \exp\left[-\int_{\Delta H}\alpha(\lambda)\,dH\right], \qquad (23)$$

while the value $\int_{\Delta H}\alpha(\lambda)dH = \tau(\lambda,\theta,\phi)$ is the optical thickness of the atmosphere in direction (θ,ϕ). To facilitate calculations, the optical thickness of a line of random slope (θ,ϕ) is usually represented in form [19]

$$\tau(\lambda,\theta,\varphi) = \tau_\lambda(0)\cdot m_\lambda(\theta,\varphi), \qquad (24)$$

where $\tau(0)$ is the optical thickness of a verticle atmospheric column of altitude ΔH_0 which is equal to a projection of section ΔH which lies with it in a verticle plane with reference to the surface the earth, and $m_\lambda(\theta,\phi)$ is the optical mass of the atmosphere.

Results of calculations show [19], that for $\theta < 60°$ refraction may be disregarded and the atmosphere considered planar-parallel, then

$$m(\theta, \varphi) = \sec \theta. \tag{25}$$

For $\theta > 60°$ $m(\theta, \phi)$ is more strictly dependent on θ [19]. In determining the optical thickness in the direction of the sun, expression (24) with the conditions in (25) takes the form

$$\tau(\lambda, \theta, \varphi) = \tau_\lambda(0) \cdot m_\lambda(z_\odot) = \tau_\lambda(0) \cdot \sec z_\odot, \tag{26}$$

where $z_\odot$ is the zenith distance of the sun.

Weakening of radiation in the atmosphere due to absorption has a spectral character which depends on quantum mechanical phenomena which occur during the oscillating-rotating movement of molecules in the atmosphere. The degree of weakening, which depends on the number of molecules absorbed in the line, depends principally on the concentration of three components: water vapor, carbon dioxide, and ozone. /21

Water vapor, which is the principal variable component of the atmosphere, absorbs radiation. The water vapor enters the atmosphere due to water evaporated from the earth's surface and is propagated through the atmosphere by mixing. It's concentration varies from zero to 2-4% depending on a series of factors, in particular, the temperature of the air and atmospheric pressure; it decreases markedly with altitude and above 10-12 km it is considered to be negligible [24, 19]. Experimental data on the water vapor concentration in the atmosphere are presented in Fig. 40. Water vapor more strongly absorbs radiation in bands centered on wavelengths λ = 0.94; 1.13, 1.38 (1.3-1.5); 1.46; 1.87, (1.7-2.0); 2.66 (2.4-3.4); 3.15; 6.26 (4.5-8.0); 11.7; 13.5; 14.3 μ m. It is also, together with CO_2, the reason for the nearly complete absorption by the atmosphere of a wide range of radiation, beginning with 15 μ m. Aside from this, the absorption bands of CO_2 are also situated near wavelengths λ = 2.05; 2.6; 4.3 (4.0-4.7) and (12.8-17.3) μ m. The volumetric concentration of CO_2 in the atmosphere is usually accepted to be constant and equal to 0.033% [8], and this composition is constant to an altitude of approximately 50 km. However, the CO_2 concentration in industrial centers of large cities may increase sharply. The distribution of ozone is not uniform by altitude; the extreme maximum value for O_3 concentration is found at an altitude of approximately 23 km, but its values depend on geographic latitude and time of year (Fig. 41). The most important bands of ozone absorption the spectral intervals under consideration are λ = 0.25 (0.2÷0.3) μ m and λ = 9.6 (9.4-9.8) μ m. Other ozone bands (4.75 and 14 μ m) are usually masked by the absorption of water vapor and CO_2. In addition to

the atmospheric components enumerated, other gases also have absorption properties, but as concerns energy, the absorption of radiation in the optical range by them is negligible and is usually not considered. Thus, the selective character of the absorption of radiation by the atmosphere, as illustrated in Fig. 42, is manifested as separate or combined intensive absorption bands, separated by transmittance apertures with insignificant absorption, which are basically in the spectral intervals 0.3 ÷ 0.93; 0.95 ÷ 1.05; 1.2 ÷ 1.3; 1.5 ÷ 1.8; 2.1 ÷ 2.4; 3.3 ÷ 4.2; 4.5 ÷ 5.0; 8 ÷ 13 μm. The quantitative determination of the degree to which radiation is weakened due to absorption on the sloped lines which interest us is related to the precise calculation of the change in the form of the absorption band with altitude and is very difficult. However, there is a series of methods which give approximate results [10, 12, 19]. /22

The extent to which radiation is scattered depends on the concentration and size of the scattered particles, and also on the relation between their size and wavelength of radiation. The relation between the scattering coefficient $\alpha_s(\lambda)$ and the length of the wave is expressed by this approximate formula [24]

$$\alpha_s(\lambda) \approx \lambda^{-\psi}. \qquad (27)$$

For particles which are small in comparison with the length of the wave $\psi = 4$ (Rayleigh scattering). With an increase in the particle size this connection is weakened and the value of ψ approaches zero (Mi scattering).

Rayleigh (molecular) scattering is always present even in a dry and pure atmosphere, while aerosol scattering is more closely connected with "optical weather" (haze, fog, etc.) and thus $\alpha_{s\lambda}$ may be conveniently considered in the form [19]

$$\alpha_s(\lambda) = \alpha_M(\lambda) + \alpha_a(\lambda), \qquad (28)$$

where $\alpha_{m\lambda}$ is the molecular scattering coefficient;
$\alpha_{a\lambda}$ is the aerosol scattering coefficient.

Calculations in [10, 19] show that Rayleigh scattering sharply reduces the intensity of directional radiation in the visible wavelength range, while with cloudless atmospheric conditions the role of Rayleigh scattering is highly significant even with pronounced aerosol turbidity in the atmosphere. In the infrared region of the spectrum for $\lambda > 1$ μm, molecular scattering may be disregarded, as it does not make a noticeable contribution to the decrease in transmittance. /23

The degree to which aerosol is diluted is related to the turbidity of the atmosphere, characterized by the meteorological

range of vision S_M in the relation [27]

$$S_M = 3{,}912 / \alpha_a(0{,}55), \quad (29)$$

where $\alpha_a(0.55)$ is the aerosol scattering coefficient for $\lambda = 0.55$ μm. By substituting the value of $\alpha_a(0.55)$ from (29) in (23) we obtain a value for the aerosol transmittance for $\lambda = 0.55$ μm [27]

$$T_a(0{,}55) = \exp\left[-3{,}912 \cdot \Delta H / S_M\right]. \quad (30)$$

Since S_M is correlated with the distribution of particles by size, it allows us to determine not only the transmittance $T_a(0.55)$, but also the spectral aerosol transmittance $T_a(\lambda)$. In particular, in fog (S_M=0.05÷1.0 km 16) the radius of the droplets is within the interval 80÷0.5 μm with the maximum distribution approximately 5÷15 μm 24 , i.e. comparable to the wavelength up to an aperture of 8÷14 μm, and thus, the aerosol dilution coefficient, determined from (29), continues to be significant in a wide spectral interval. Thus, remote investigations of the earth's surface with optical-electrical instruments are impossible at the distances of interest to us through fog and solid clouds.

The above allows us to limit the possible atmospheric conditions of haze and fog in further observations, i.e. in the presence of aerosol in sizes to 1.0 μm ($S_M > 1.0$ km). In [8] it was shown that with an approximation of the real distribution of the concentration of aerosol particles in sizes from 0.1 to 1.0 μm, /24
depending on altitude, aerosol dilution may have practical interest only in the lower 5-km layer of the atmosphere with an exponential reduction in the concentration of particles with altitude. On the basis of a comparison of the aerosol scattering and absorption factors in the decrease in radiation we concluded that in the presence of atmospheric haze and with average visibility (S_M = 10 km), aerosol dilution in the lower 5 km layer of the atmosphere in the wavelength interval 2.5÷14 μm is negligible in comparison to the absorption of water vapor and CO_2. In the spectral interval to 2.5 μm, the aerosol dilution factor must be considered.

The process of scattering emitted radiation in the atmosphere influences not only the degree to which a direct flow of radiation is diluted, but also produces an additional component which results in its multiple participation in the transfer process. This added component evidently affects the conditions of irradiation of the observed object by an external irradiator, as well as the irradiance input to the pupil of the probing system, thus producing a so-called "atmospheric haze". The brilliance of this haze in a direction (θ, ϕ) depends not only on the atmospheric condition and the scattering and absorbing properties of its components, but also on the situation and brilliance of the external

irradiator and the albedo of the underlying surface. Computing the parameters of the atmospheric haze to one or another approximation is usually done on a determined model of the atmosphere, for example one of those suggested in [22, 27].

Aside from sound irradiance, which is produced by radiative currents of atmospheric haze in those spectral intervals where scattering is perceptible, the atmosphere produces sound due to its inherent thermal radiation. Since, as was said above, for $\lambda > 2.5 \div 3$ μm there is little scattering, it is usually disregarded in considering the process of the transfer of thermal radiation in a cloudless atmosphere [12]. Another very important simplification used here is the hypothesis of the existence of a local thermodynamic equilibrium [12]. Following from this, the inherent radiation coefficient for the atmosphere $\varepsilon(\lambda)$ does not depend on the intensity of transmitted radiation, and Kirchhoff's law holds and is given in the form /25

$$\varepsilon_a(\lambda) = \alpha_a(\lambda). \tag{31}$$

On the basis of data on the distribution of atmospheric temperatures T_a and the absorption coefficient $\alpha_a(\lambda)$ along a line of length ΔH, the intensity of atmospheric radiation in the direction (θ, ϕ) of this line is described by the relation

$$B_h(\lambda,\theta,\varphi) = \int_{\Delta H} \varepsilon_a(\lambda) \cdot B_\lambda^{ABS}(T_a) \cdot \exp\left[-\int_{\Delta H} \alpha_a(\lambda)\, dH\right] dH, \tag{32}$$

where $B_\lambda^{ABS}(T_a)$ is the spectral brilliance of an absolutely black substance at atmospheric temperature T_a.

Thus, the observed properties of the earth's atmosphere and the character of the transfer of radiation which depends on them show that results of distance measurements of the spectral brilliance of a concrete object may actually be determined not only by the optical characteristics of the object and of external irradiators, but also by the relation between a series of secondary radiation currents which are shown conditionally in Fig. 43. Considering the above and following from [11, 27], we present the observed brilliance of a given object in the form

$$B(\lambda,\theta,\varphi) = B_0(\lambda,\theta,\varphi) \cdot T(\lambda,\Delta H) + B_h(\lambda,\theta,\varphi), \tag{33}$$

where $T(\lambda, \Delta H)$ is the transmitting of atmospheric radiation on the line between the object and the measuring system which is at a distance ΔH from the object in direction $(\theta\ \phi)$, and $B_h(\lambda, \theta\ \phi)$ is the brilliance of the atmospheric haze caused by scattering and/or inherent radiation in the atmosphere in the same direction. Relation (33) is more useful in a quantitative analysis of the effect of the atmosphere on results of remote measurements, since

it directly describes the transformation from surface brilliance to the brilliance measured by the probing system. This transformation, in accordance with the above information, is most perceptible in absorption bands and in high scattering regions, as illustrated in Fig. 44,...47. We note, in particular, the significant increase in sound brilliance in short wave regions which corresponds to a a significant amount of Rayleigh scattering and to a sharp change in observed brilliance temperatures close to absorption bands due to the redistribution of radiation currents from the earth's surface and from the cold upper layers of the atmosphere in favor of the latter. /26

To describe the degree of transformation of atmospheric brilliance $B_0(\lambda, \theta, \phi)$ to brilliances $B(\lambda, \theta, \phi)$ we use the transmission function $\Pi(\lambda, \theta, \phi)$ proposed in [11, 12], the relation

$$B_0(\lambda, \theta, \varphi) = \Pi(\lambda, \theta, \varphi) \cdot B(\lambda, \theta, \varphi), \tag{34}$$

considering (33) reduced to the form [11]

$$\Pi(\lambda, \theta, \varphi) = \left[\left(1 + \frac{B_h(\lambda, \theta, \varphi)}{B_0(\lambda, \theta, \varphi) \cdot T(\lambda, \Delta H)}\right) \cdot T(\lambda, \Delta H)\right]^{-1}. \tag{35}$$

As seen from this expression, the theoretical determination of the transmission function of the atmosphere is a problem which comprises all of the current problems in transfer theory, and as such may be done with precision, defined by the selected atmospheric model, only for some special conditions and approximations [19, 22, 27]. The transmission function of the atmosphere can also be determined experimentally [11]. We suggest that the investigated subject represents object C_K with small linear size on the background of object C_L or of two homogeneous half planes C_K and C_L. Recording relation (33) for each of the objects for conditions under which the area of the small object C_K is several times larger than the instantaneous visual field of the probing system, we obtain this system of equations /27

$$\begin{cases} B_K(\lambda, \theta_K, \varphi_K) = B_h^K(\lambda, \theta_K, \varphi_K) + B_0^K(\lambda, \theta_K, \varphi_K) \cdot T(\lambda, \theta_K, \varphi_K) \\ B_L(\lambda, \theta_L, \varphi_L) = B_h^L(\lambda, \theta_L, \varphi_L) + B_0^L(\lambda, \theta_L, \varphi_L) \cdot T(\lambda, \theta_L, \varphi_L). \end{cases} \tag{35}$$

Considering that near to the interface of objects C_K and C_L, the optical properties of the atmosphere do not change in the horizontal direction, we may consider that for measurements near the interface under conditions where $\theta_K = \theta_L$ and $\phi_K = \phi_L$ that

$$\left.\begin{aligned} T(\lambda, \theta_K, \varphi_K) = T(\lambda, \theta_L, \varphi_L) = T(\lambda, \theta, \varphi) \\ B_h^K(\lambda, \theta_K, \varphi_K) = B_h^L(\lambda, \theta_L, \varphi_L) = B_h(\lambda, \theta, \varphi) \end{aligned}\right\} \tag{36}$$

and while the brilliance value for haze $B_h(\lambda, \theta, \phi)$ will correspond to that value for some average value of the optical characteristics of the subject. Then from (35) we get

$$T(\lambda,\theta,\varphi)=\frac{B_K(\lambda,\theta,\varphi)-B_4(\lambda,\theta,\varphi)}{B_o^K(\lambda,\theta,\varphi)-B_o^4(\lambda,\theta,\varphi)} \tag{36}$$

and

$$B_h(\lambda,\theta,\varphi)=B_K(\lambda,\theta,\varphi)-B_o^K(\lambda,\theta,\varphi)\cdot T(\lambda,\theta,\varphi)$$

Thus, for known surface brilliances $B_o(\lambda, \theta, \phi)$ for selected pairs of objects and subject, it is possible to determine the transmission function of the atmosphere on the basis of measurements of the corresponding observed brilliances $B(\lambda, \theta, \phi)$. We would like to emphasize that terrestrial measurements on polygons which are synchronous or quasi-synchronous with measurements taken from aerospace platforms conform to these conditions. An example of a similar determination of the components of the transmission function based on results of spectrometry of the earth's surface with pilot channel receiver "Soyuz-7" is illustrated in Fig. 48. /28
Of course one of several artificial gages may be used in this method. In particular, a surface gage such as a special mirror [32] with brilliance $B_m(\lambda, \theta, \phi)$, as compared to the brilliance of the surrounding natural environment $B_e(\lambda, \theta, \phi)$, and with an area which is negligible in comparison to the instantaneous field of vision of the probing system, is of significant practical interest. For this case, relation (33) is comprised of the following system of equations:

$$\begin{cases} B_e(\lambda,\theta_e,\varphi_e)=B_h^e(\lambda,\theta_e,\varphi_e)+B_o^e(\lambda,\theta_e,\varphi_e)\cdot T(\lambda,\theta_e,\varphi_e) \\ B_g(\lambda,\theta_g,\varphi_g)=B_h^g(\lambda,\theta_g,\varphi_g)+[B_o^e(\lambda,\theta_g,\varphi_g)+B_m(\lambda,\theta_g,\varphi_g)]\cdot T(\lambda,\theta_g,\varphi_g) \end{cases} \tag{37}$$

where $B_g(\lambda, \theta, \phi)$ corresponds to the observed brilliance in direction (θ_g, ϕ_g) of the platform holding the gage. Solving this system while considering the conditions in (36) we find

$$T(\lambda,\theta,\varphi)=T(\lambda,0)^{\exp[\sec\theta]}=\frac{B_e(\lambda,\theta,\varphi)-B_g(\lambda,\theta,\varphi)}{B_m(\lambda,\theta,\varphi)}, \tag{38}$$

or, considering (24) and (25) and also that

$$B_m(\lambda,\theta,\varphi)=\tilde{r}_m(\lambda,\theta,\varphi)\cdot E_\odot\cdot\cos z_\odot\cdot\exp[\tau_\lambda(0)\cdot\sec z_\odot], \tag{39}$$

we get

$$T(\lambda,0)=\frac{B_e(\lambda,\theta,\varphi)-B_g(\lambda,\theta,\varphi)}{\tilde{r}_m(\lambda,\theta,\varphi)\cdot E_\odot\cdot\cos z_\odot\cdot\exp[\sec z_\odot+\sec\theta]}. \tag{40}$$

From the deduced relation it follows that to determine an important parameter of the atmosphere such as its transmittance in a vertical direction, a gage of small dimensions (for which $r_m(\lambda, \theta, \phi)$, naturally, is known) is sufficient. In this case, /29
if an active irradiator, such as a projector, is used, relation (38) may be used to determine $T(\lambda, 0)$.

The limiting condition of the experimental methods discussed above which determine the transmission function of the atmosphere and its components is the difference in values for the brilliance

of haze B_h^K and B_h^L or B_h and B_h which emerge in data from remote measurements of objects in a single direction (θ, ϕ) which are separated from the interface by a distance exceeding the flight altitude for airplane measurements or the altitude of the uniform atmosphere for satellites [9]. We also note that in determinations of the transmission function for the spectral interval of inherent radiation in the absence of scattering, both components $T(\lambda, \theta, \phi)$ and $B_h(\lambda, \theta, \phi)$ will depend only on the concentration and distribution of absorbed components in the atmosphere. In particular, for the transmittance aperture $8 \div 12\ \mu$ m, absorption by water vapor predominates, thus, for practical purposes the transmission function is determined only from the moisture content of the atmosphere (Fig. 49) [10].

The properties and characteristics of the atmosphere referred to above concern basically its momentary condition. However, it is well known that the earth's atmosphere is optically unstable and that its properties change over time and space. Thus, a significant amount of work has been devoted to the study of statistical characteristics of the atmosphere and we have been limited in selecting times for remote surveys only by the necessity of considering characteristic seasonal and diurnal variations in the transmittance of the atmosphere [28, 29]. We also note the possibility of perceptible fluctuations, resulting from the turbulence of the atmosphere, showing up in brilliance measurements.

In summary, we note first of all the significant variation in the spectral-brilliance characteristics of natural phenomena which result from their properties and conditions and which illustrate the great potential possibilities for using multispectral remote probes. On the other hand, the characteristics of these concrete objects have not been studied completely and while the volume of information about them has increased recently, local measurements and surveys of, for example, terrestrial conditions will not make them satisfactorily complete. In light of this we believe that the necessary basis for developing methods and instruments for remote sensing is a mass of a priori data on the statistical characteristics of a large number of types of natural objects which can and must emerge from remote probing from airplanes and space vehicles. As we have shown, it is entirely possible to reduce and compare results of remote and terrestrial measurements and studies. The rapid increase in the volume of data obtained in this way will lead to effective refinements in the remote sensing model.

/30

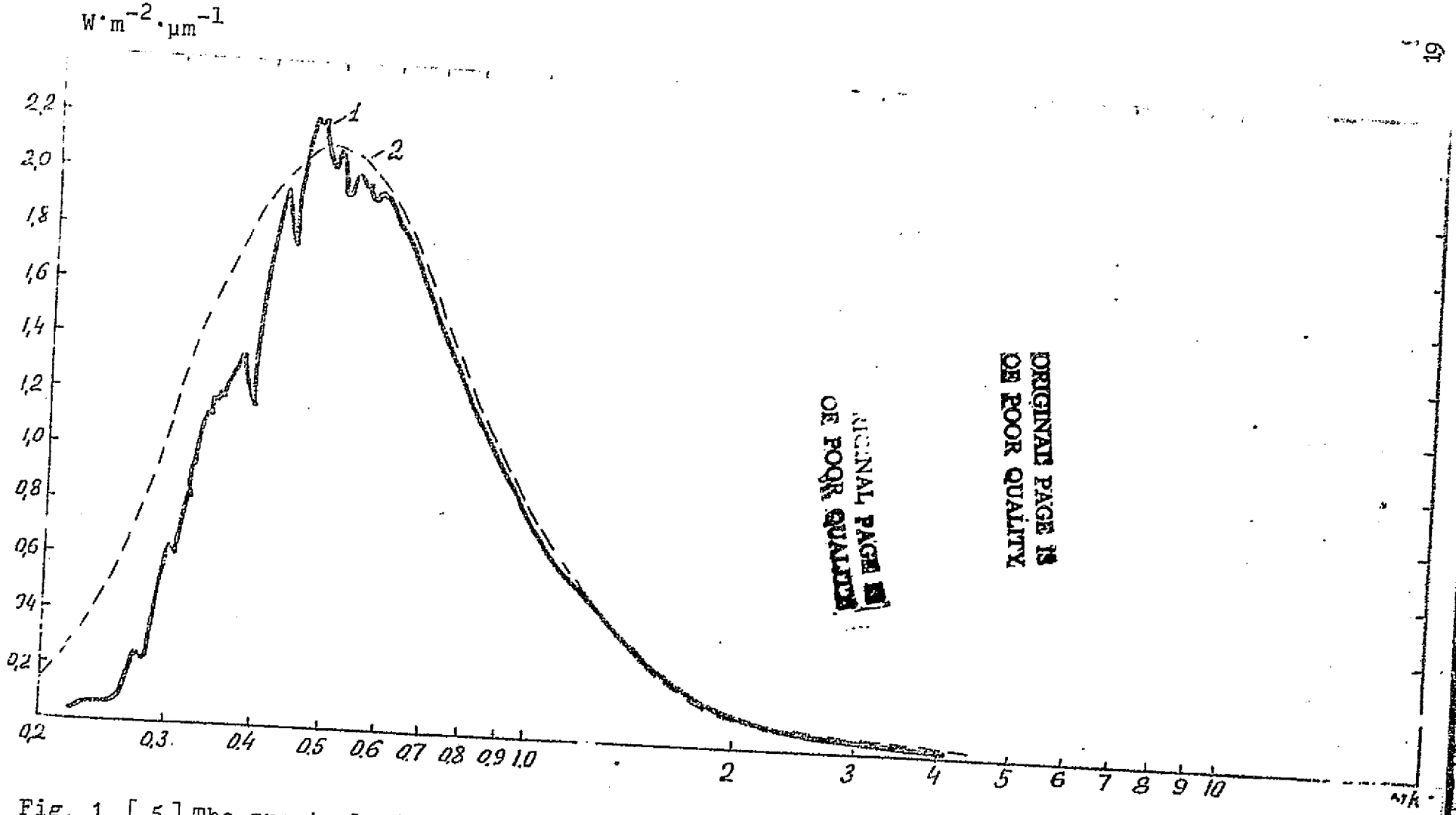

Fig. 1. [5] The spectral distribution of a normal density direct solar radiation current on the upper limit of the earth's atmosphere (1) and the temperature of an absolutely black substance of 6000 K (2).

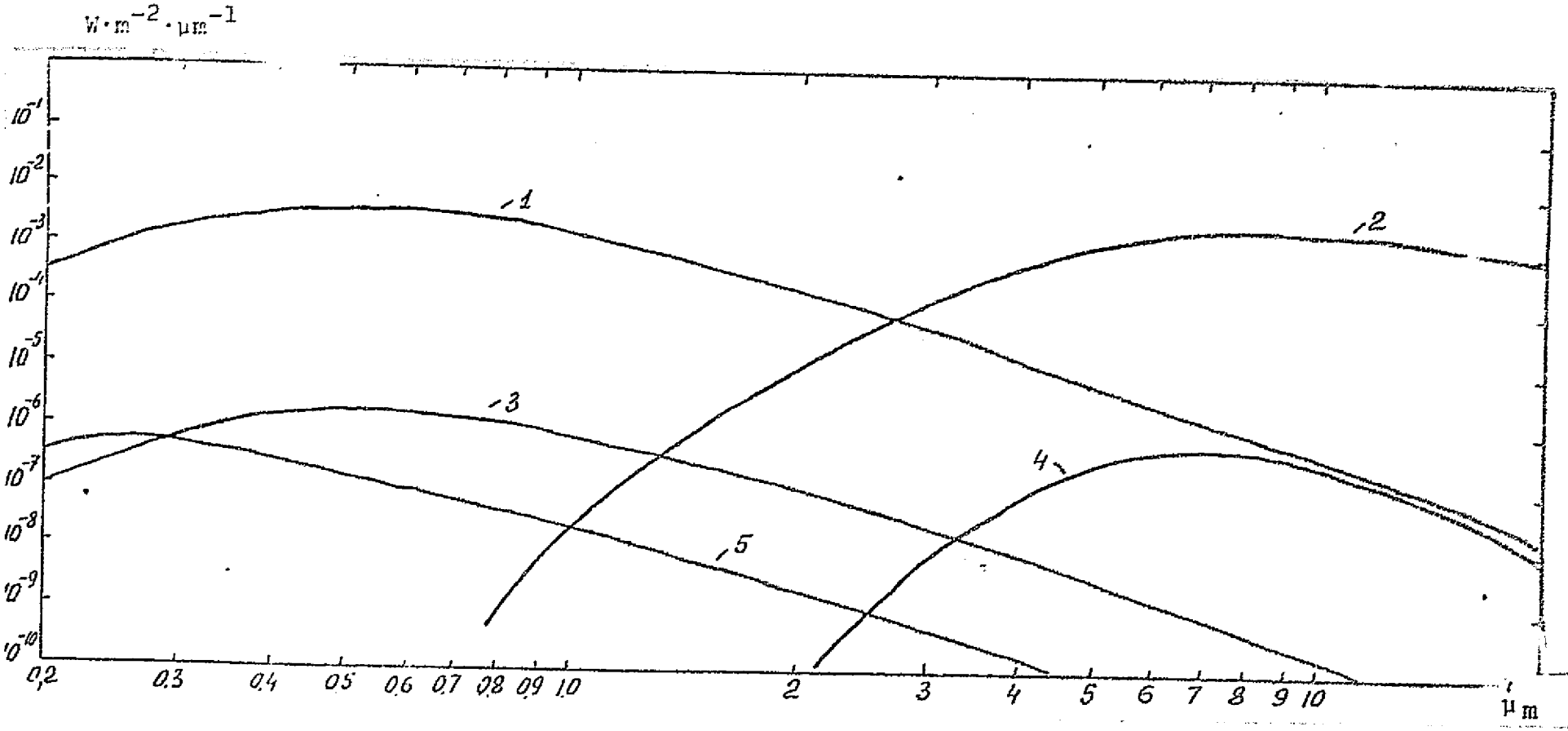

Fig. 2. The spectral distribution of a normal density direct radiation current: 1- Full moon (reflected radiation) [14]; 2- Moon (inherent radiation) [24]; 3- Venus (reflected radiation) [21]; 4- Venus (inherent radiation) [24]; 5- Sirius [24].

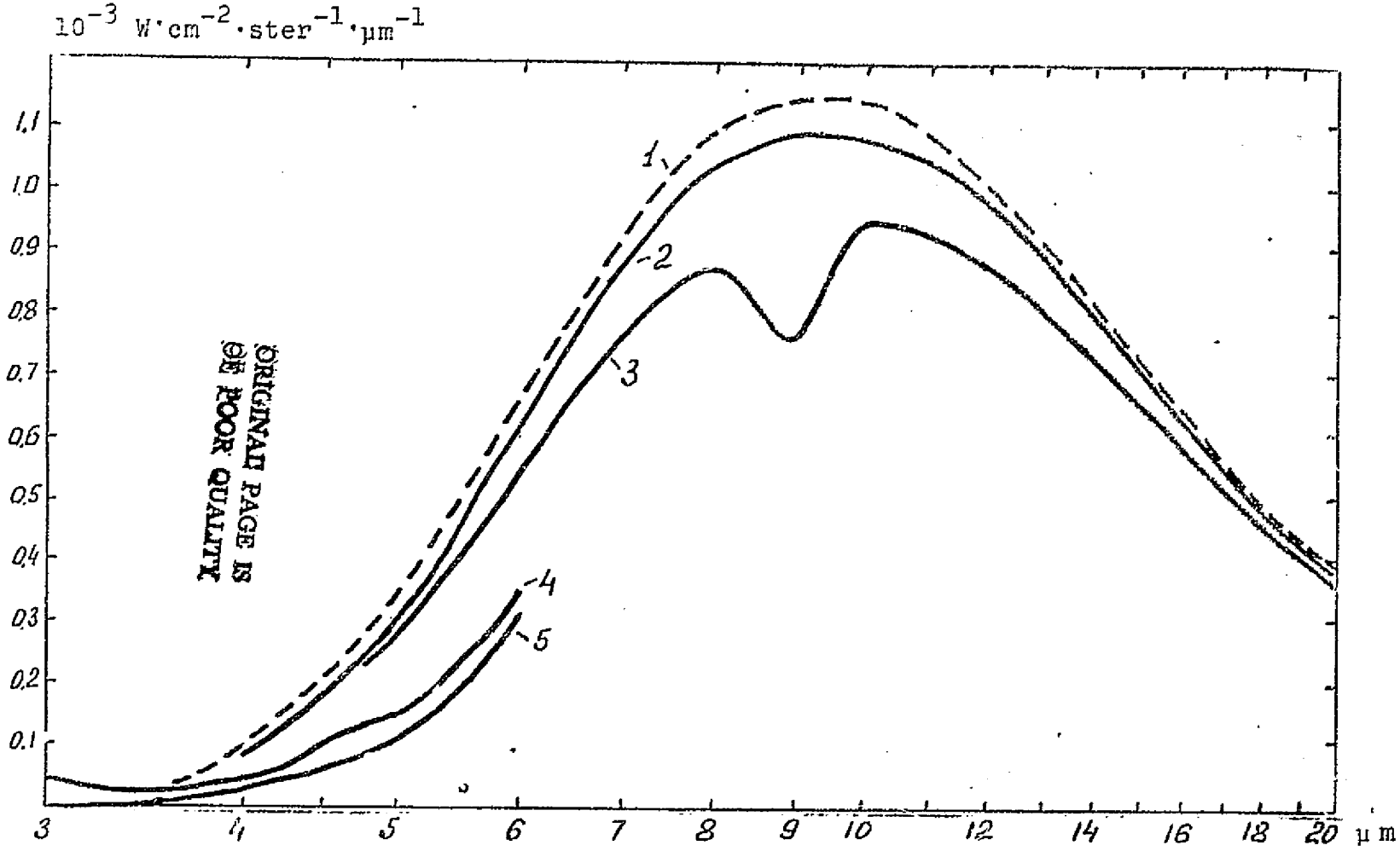

Fig.3 [24] Spectral brilliance of typical terrestrial formations observed during the day: 1- black substance, 308 K; 2- soil, 305 K; 3-white sand; 4- snow; 5- grass.

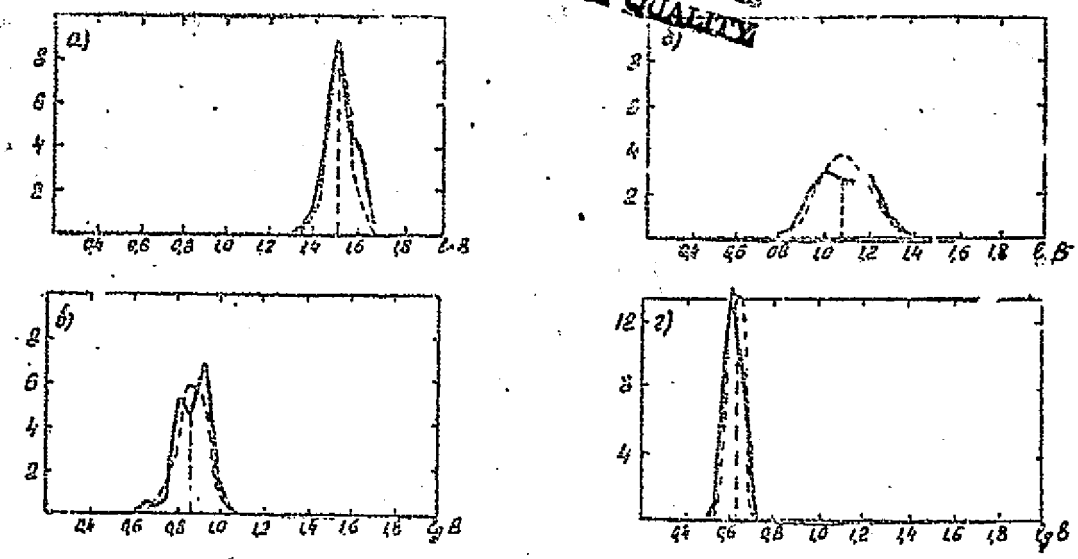

Fig. 4. [20] Distribution of probable brilliance values ($\Delta\lambda$= 0,55÷0,70 μm): a) soil ($\bar{\varphi}_a$ =1,510; $\bar{\varepsilon}$ =0,050); b) forests ($\bar{\varphi}_B$ =1,054; $\bar{\sigma}$ =0,118) ; c) meadows ($\bar{\varphi}_B$ =0,636; $\bar{\sigma}$ =0,070); d) water surfaces ($\bar{\varphi}_B$ =0,634; $\bar{\sigma}$ =0,026).

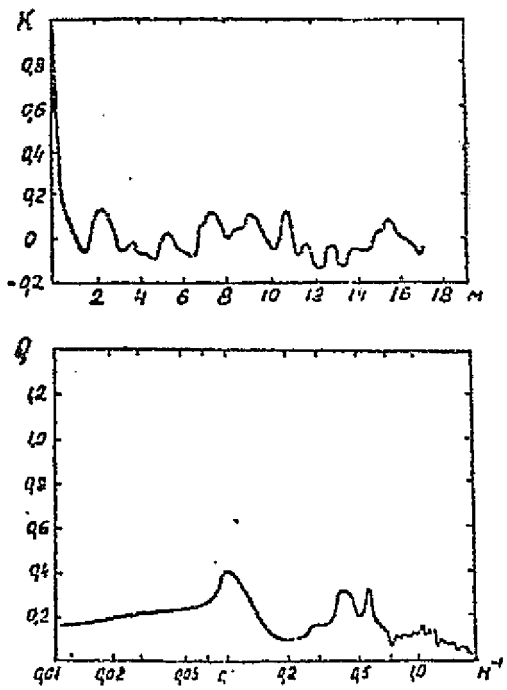

Fig. 5. [20] K(ℓ) and Q(Ω) of fresh-plowed field ($\Delta\lambda$ =0,55÷0,70 μm).

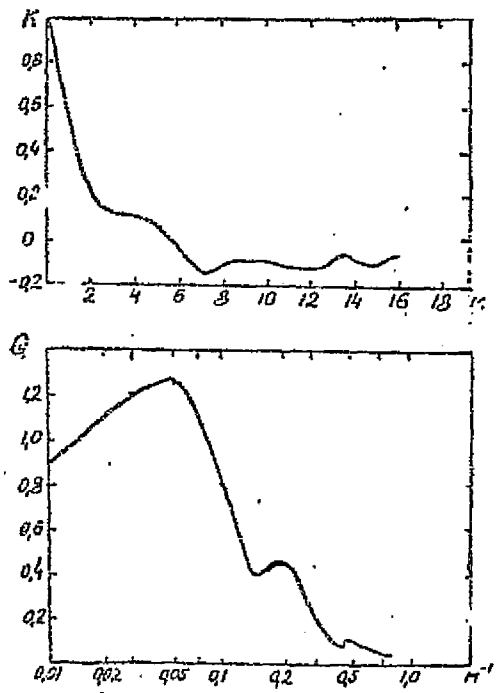

Fig. 6. [20] K(ℓ) and Q(Ω) for a field of stubble wheat 15-20 cm high, with white patches of blooming daisies ($\Delta\lambda$ =0,55+0,70 μ м).

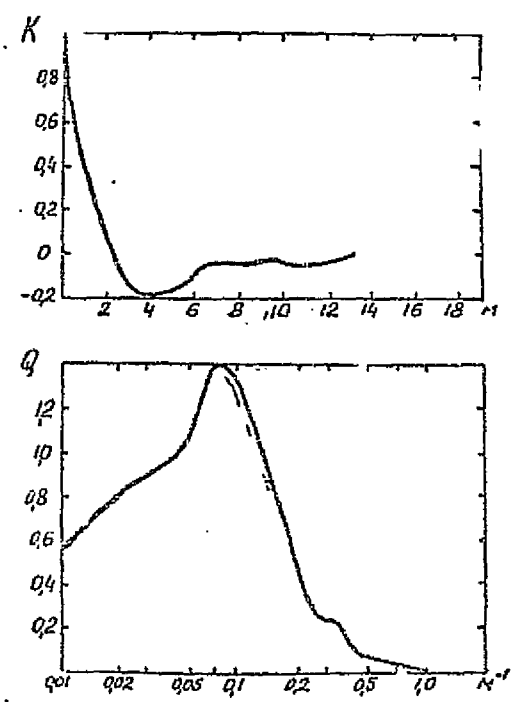

Fig. 7.[20] K(ℓ) and Q(Ω) of an oak grove with birch and aspens ($\Delta\lambda$ =0,55+0,70)

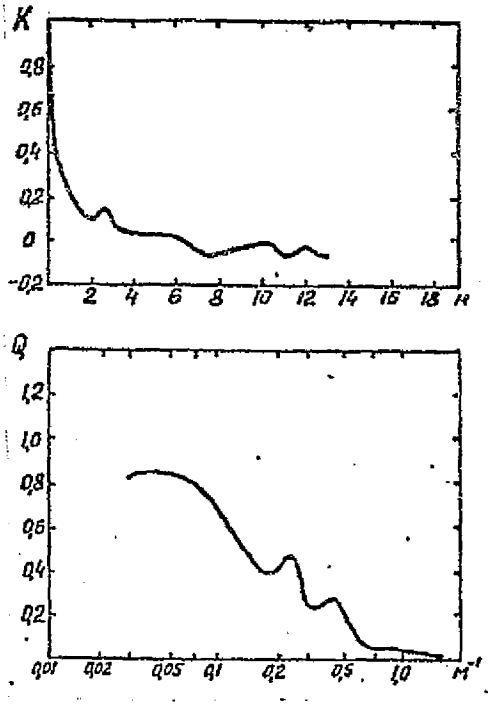

Fig. 8. [20] K(ℓ) and Q(Ω) of a mowed meadow of various grasses and word illegible ($\Delta\lambda$ =0,55÷0,70 μm).

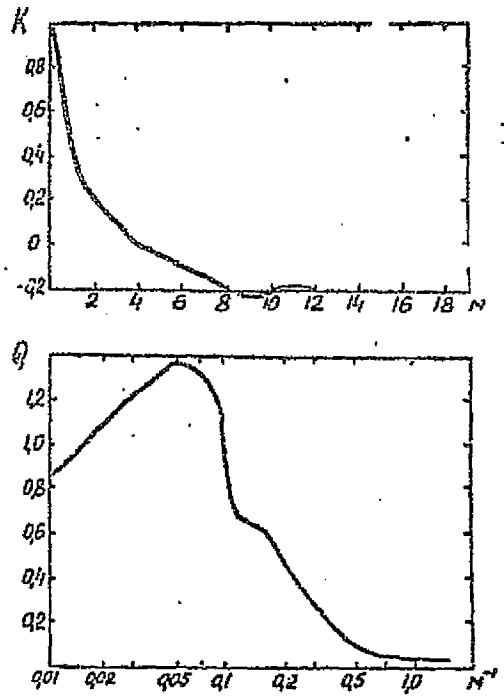

Fig. 9. [20] K(ℓ) and Q(Ω) for a low-land swamp ($\Delta\lambda$ =0,55÷0,70).

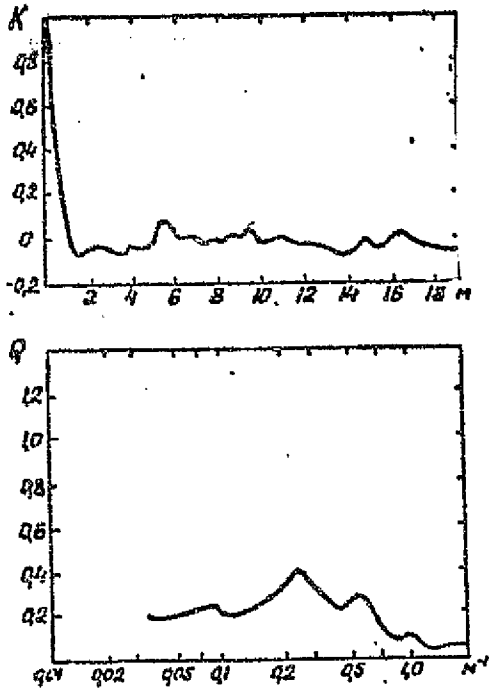

Fig. 10 [20] K(ℓ) and Q(Ω) for a calm water surface (λ = 0,55÷0,70).

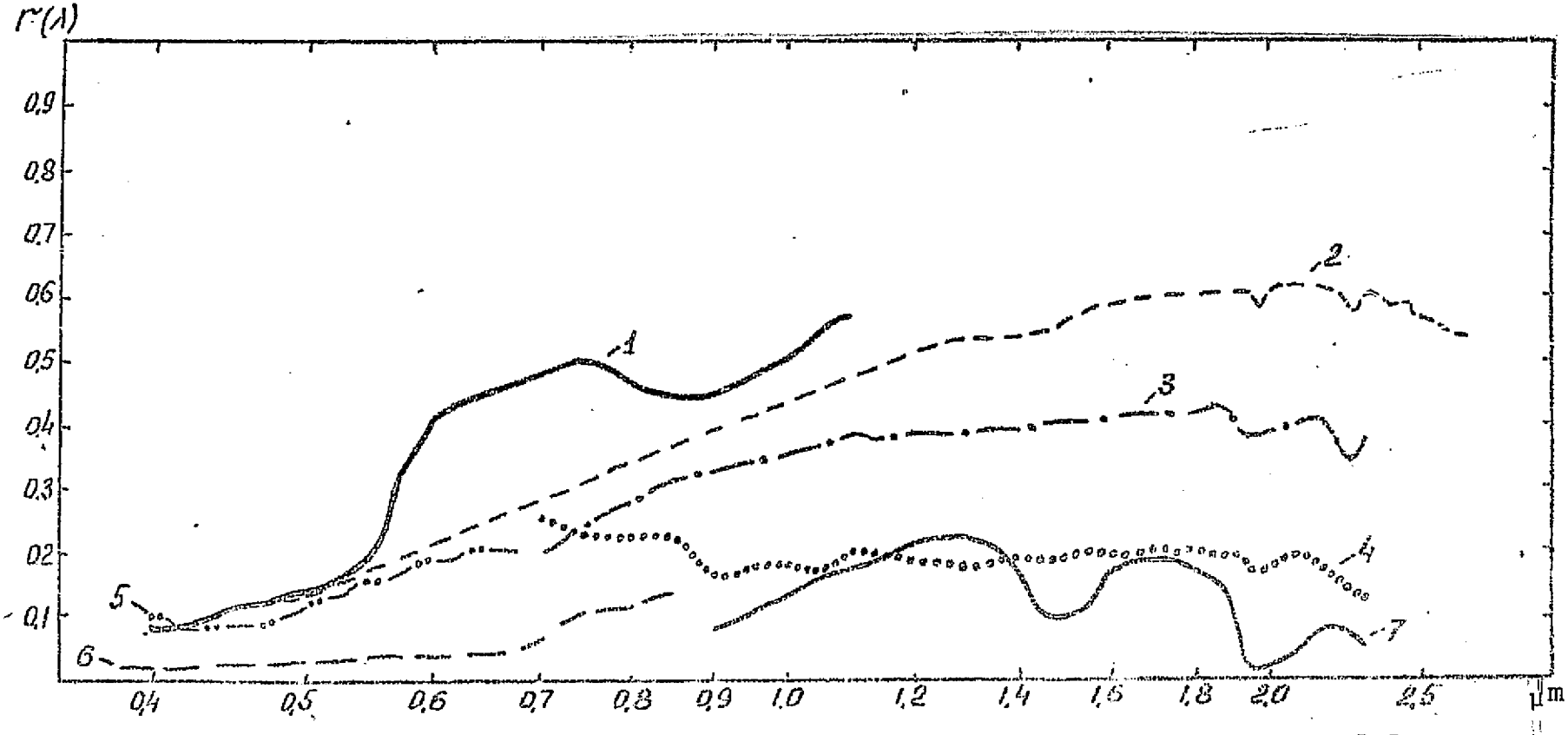

Fig. 11. Spectral brilliance coefficients for 1- red clay [7]; 2-muddy loam, dry [9]; 3-fine sand [13]; 4- concrete slabs [13]; 5- quartz sand [17]; 6- a peat bog [15]; 7- black peat, damp [13].

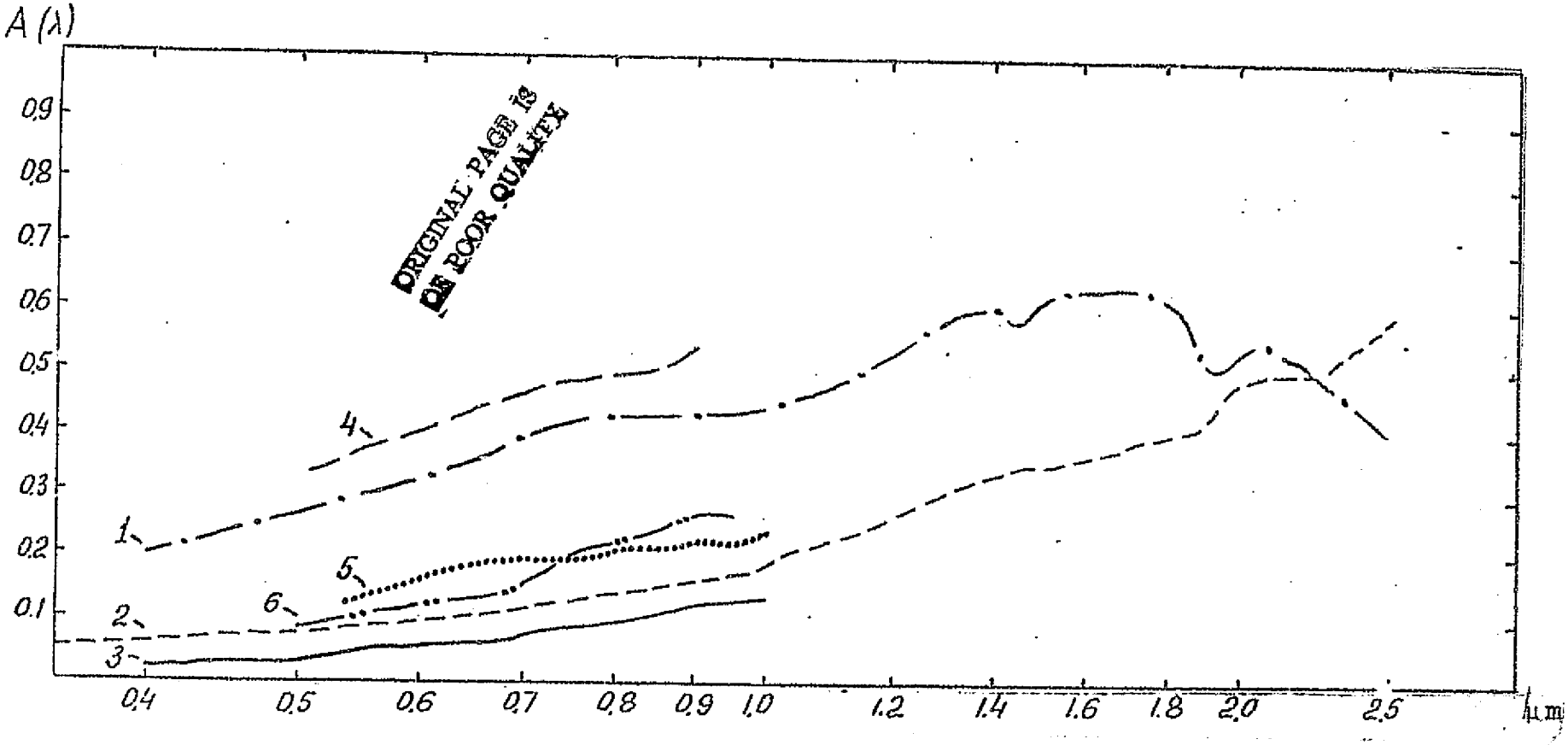

Fig. 12. Spectral albedo of: 1- sandy beach [39]; 2- loam[39]; 3- black earth, Z_0 = 42° [19] 4- white sand, fluvial, Z_0=43°[19] 5- alphalt road, Z_0=42°[19]; 6-dirt road, dry, Z_0=40° [19].

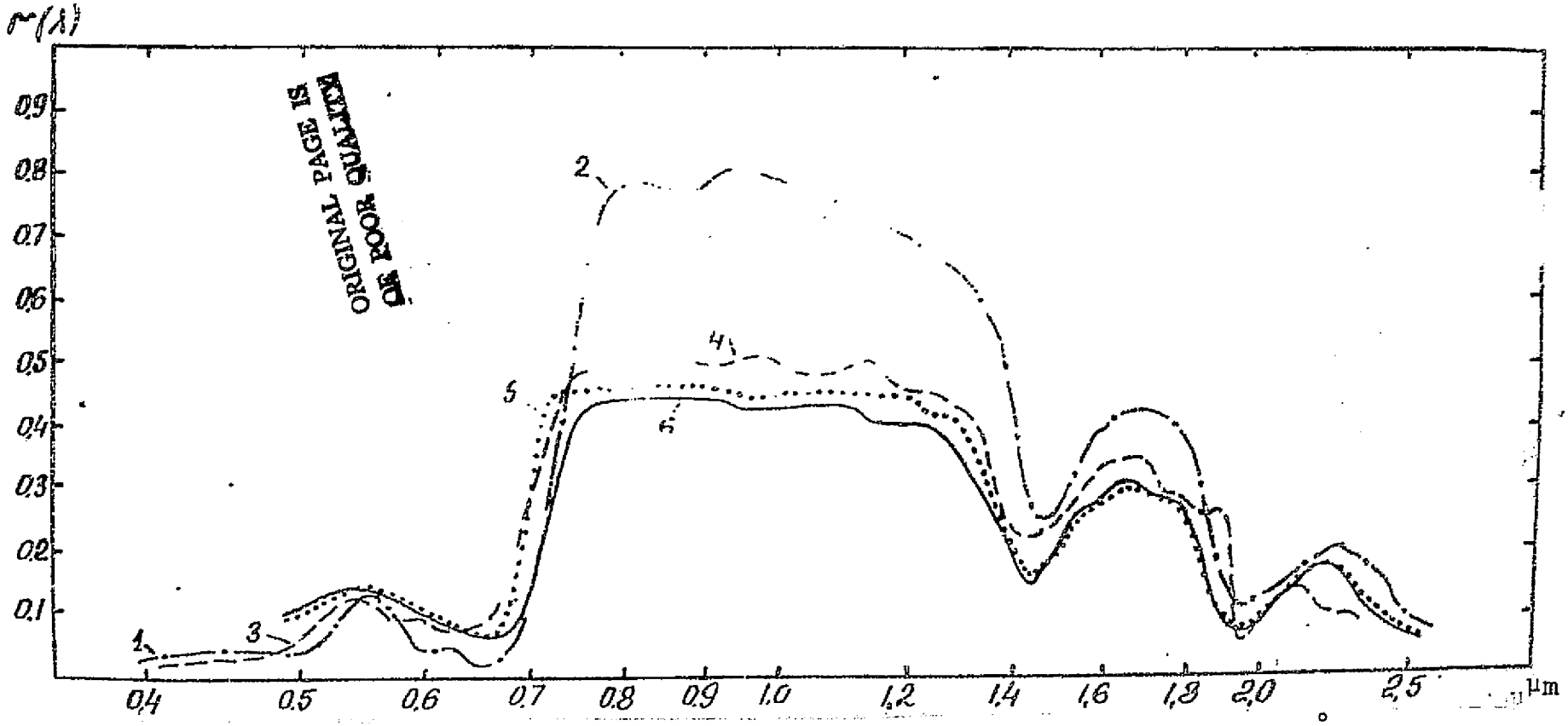

Fig. 13. Spectral brilliance coefficients of: 1- grass [15]; 2- meadow grass, mowed [13]; 3- birches [15]; 4- birch leaves [13]; 5- cotton leaves [33]; 6- corn leaves [33].

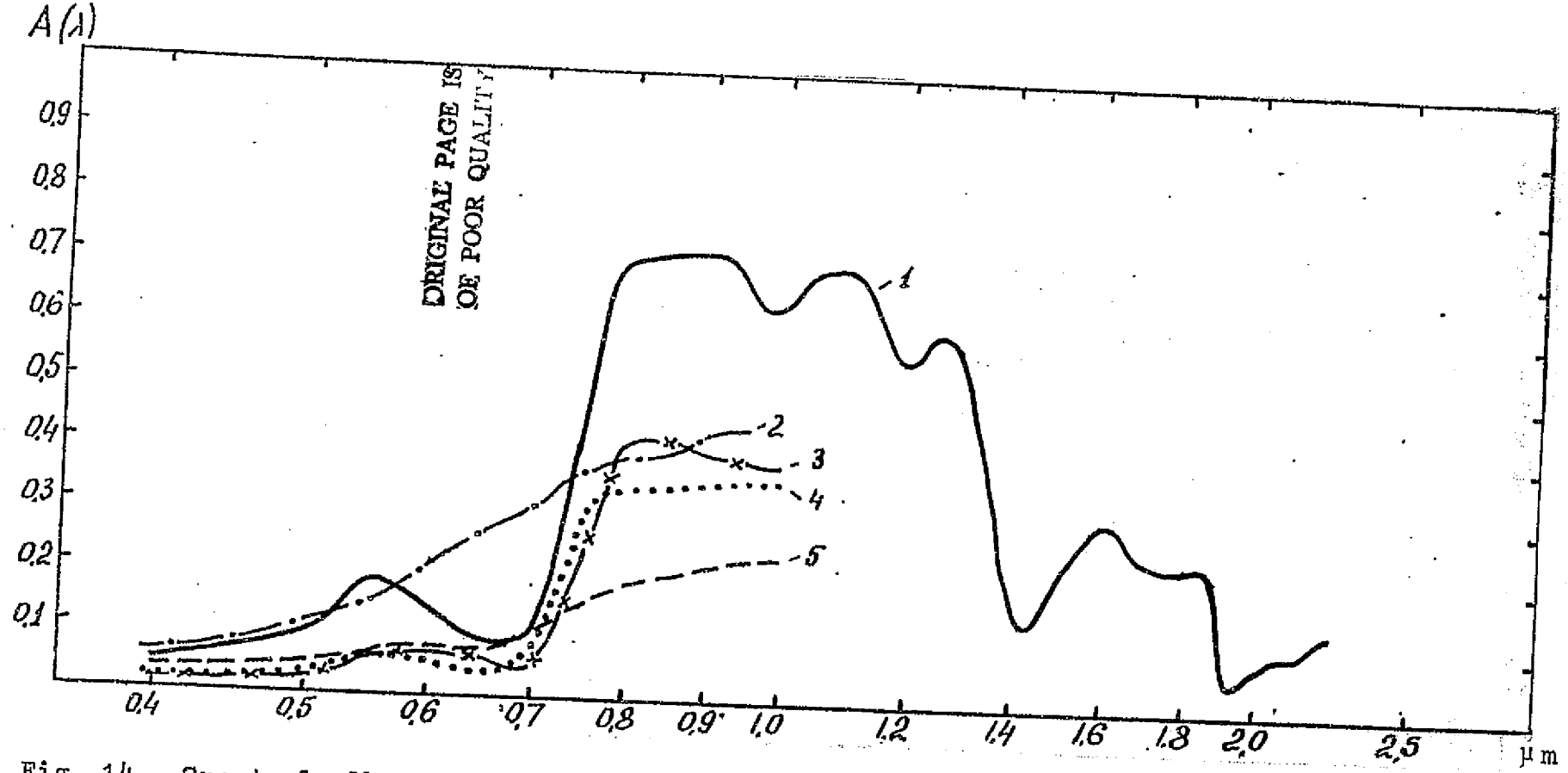

Fig. 14. Spectral albedo of: 1-pines [37]; 2- straw, Z_0=34° [19]; 3- yellow grass, thick, Z_0=34°[19]; 4-silage corn, Z_0=36°[19]; 5- sprouts of winter wheat, Z_0=42° [19].

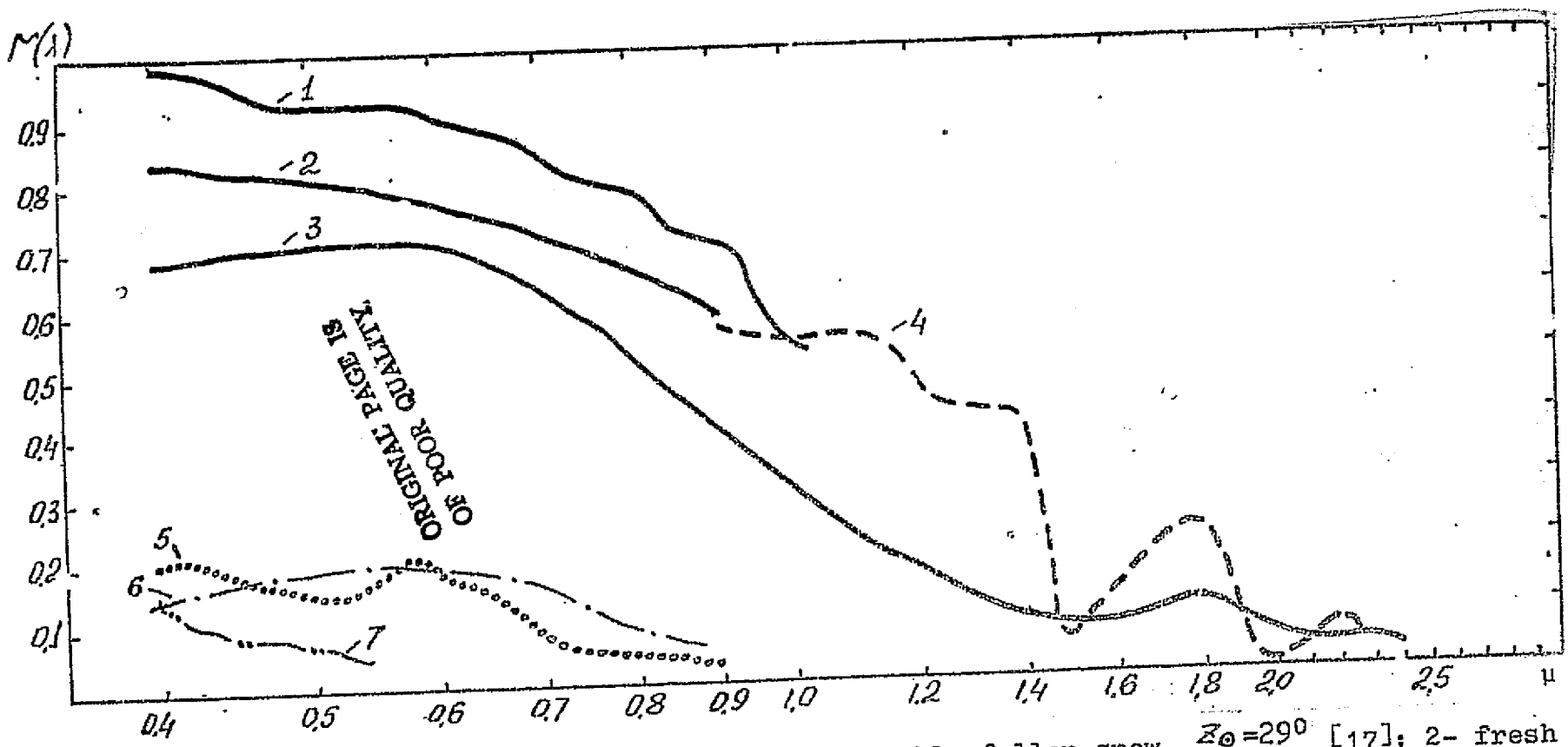

Fig. 15. Spectral brilliance coefficients of: 1- freshly fallen snow, $Z_{\odot}=29^{0}$ [17]; 2- fresh snow [15]; 3-fresh snow [13]; 4-old snow [13]; 5-water in the Gulf of Kara-Bogaz-Gol [9]; 6-water in Kubani River, turbid [15]; 7- water in a clean pond [15].

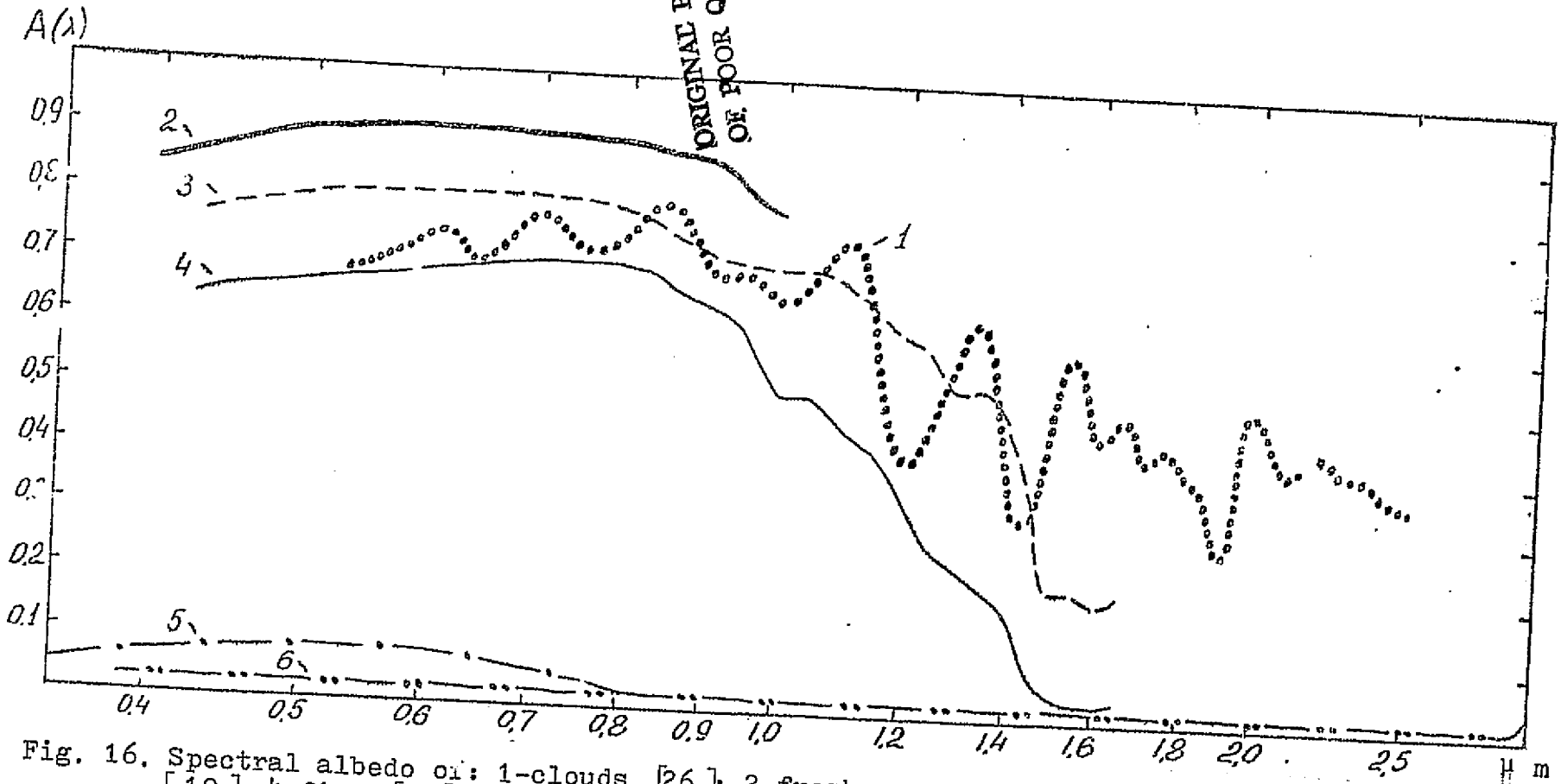

Fig. 16. Spectral albedo of: 1-clouds [26]; 2-fresh snow, dry, $z_\odot = 60^0$ [19]; 3-damp snow [19]; 4-firn [19]; 5-aqueous lake surface $z_\odot = 34^0$ [19]; 6-water surface $z_\odot = 40^0$, calculated data [19]

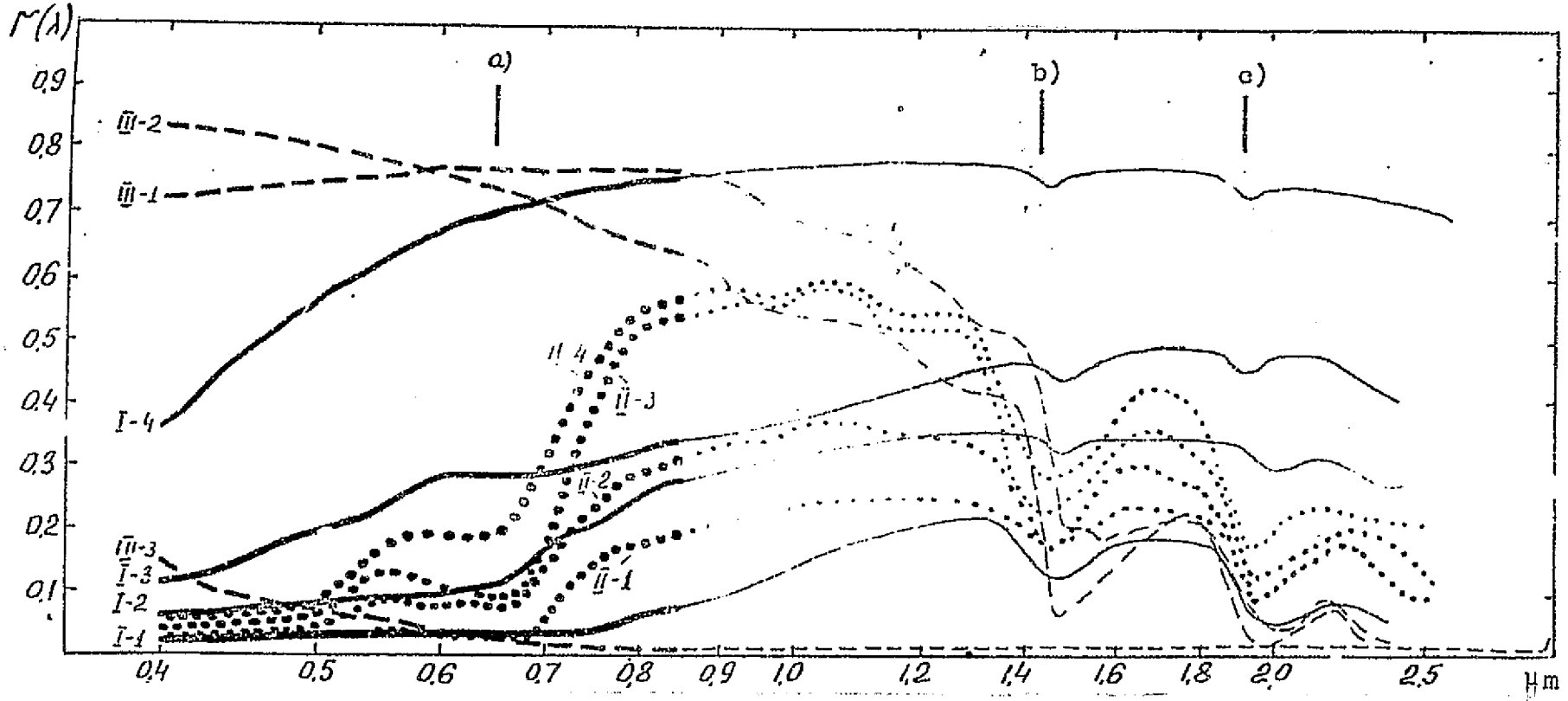

Fig. 17. Spectrophotometric classification of natural formations (according to Ye. L. Krinov). CLASS I. Outcrops and soil. Type 1-black earth soil and sandy loam, dirt roads, etc.; Type 2-podsolized loamy soil, paved roads, several types of construction; Type 3-sand, desert outcrop, rocks; Type 4-limestone, clay, various light objects. CLASS II. Plants. Type 1 and Type 2-forest conifer species in winter and summer; Type 3-dry valley meadows, grass species without sufficient succulence; Type 4-forest plants with autumn coloring and maturing (yellowing) field crops. CLASS III. Water surfaces and snow coverings. Type 1-snow covered with an ice crust; Type 2-fresh fallen snow; Type 3-water surfaces.
a) the absorption band of chlorophyll (0.64÷0.68 μm): b) and c) absorption bands of water (1.43 and 1.93 μm).

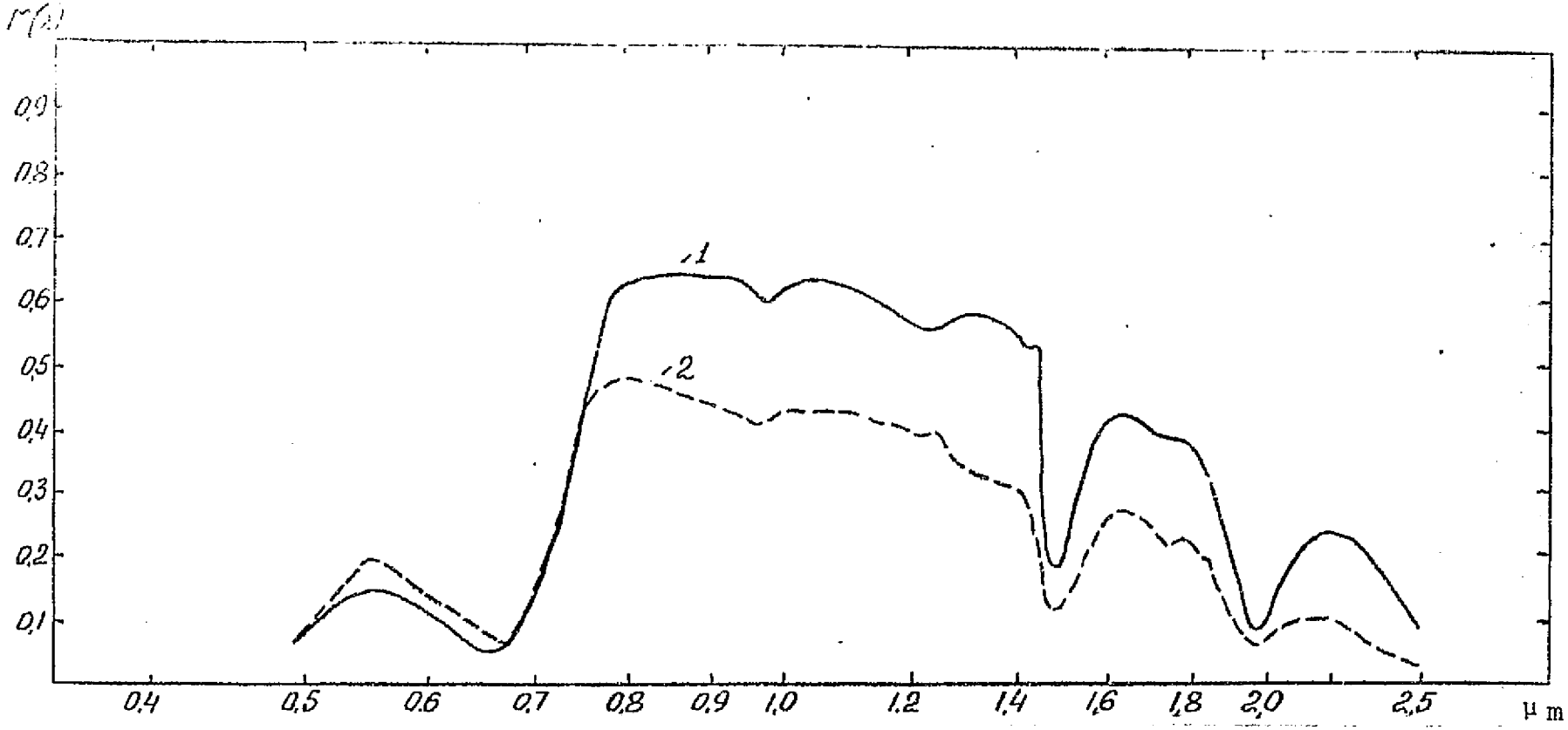

Fig. 18. [33] Spectral brilliance coefficients of citrus leaves: 1-young; 2-ripe.

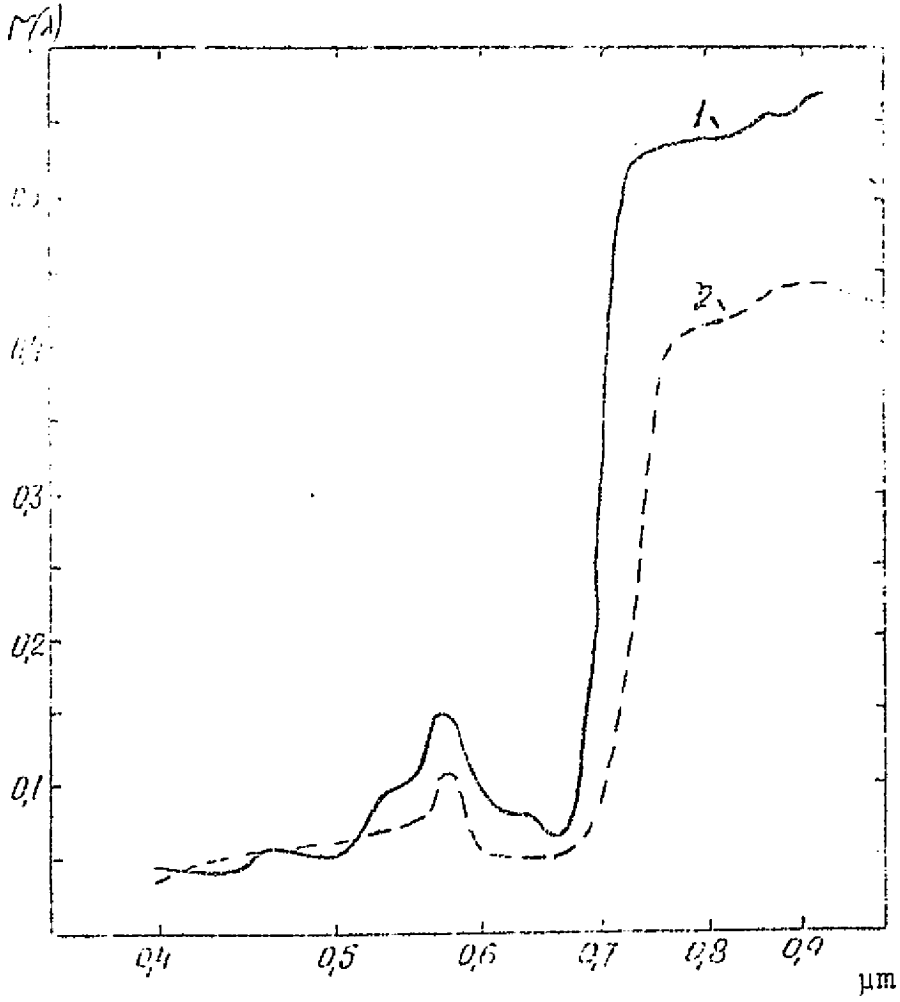

Fig. 19. [17] Spectral brilliance coefficients of cotton plants in stages of blooming and boll formation: 1-August 5, 1965, $z_0=31°$ 2-August 18, 1965, $z_0=30°$.

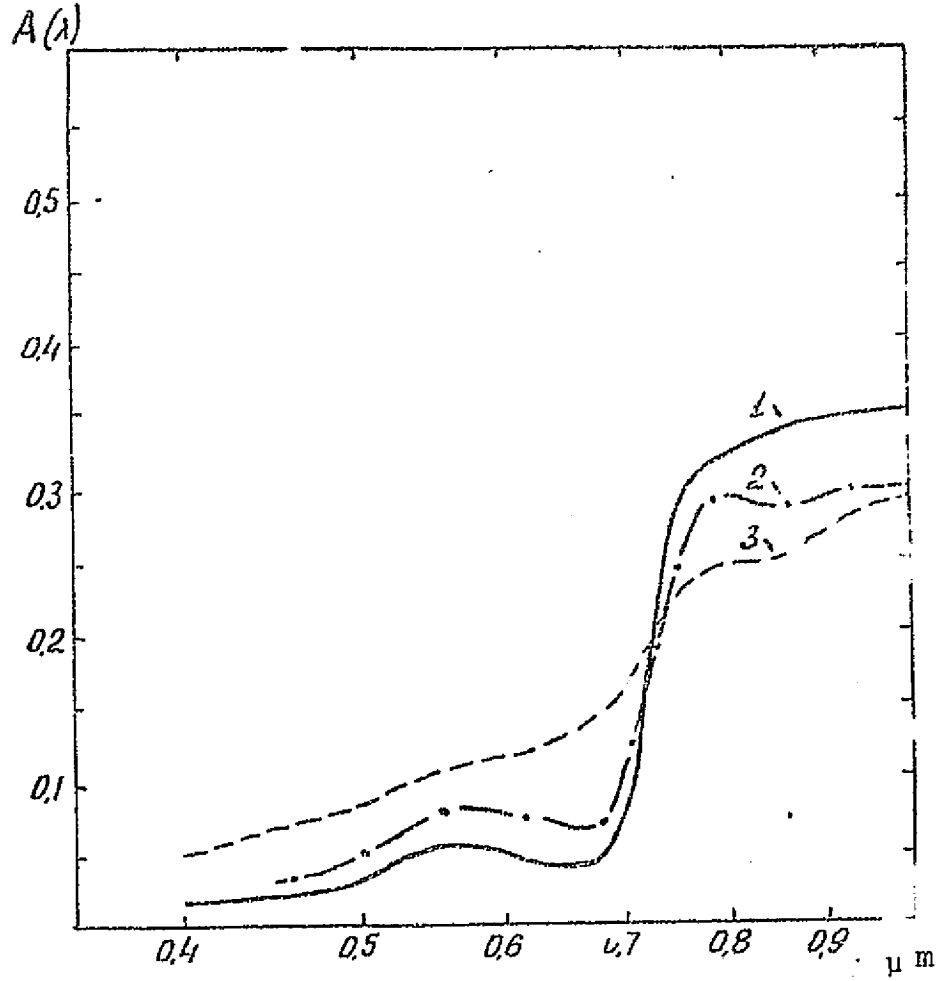

Fig. 20. [19] Spectral albedo of: 1-silage corn, $z_0=36°$; 2-high green corn, $z_0=34°$; 3-yellow corn, $z_0=44°$.

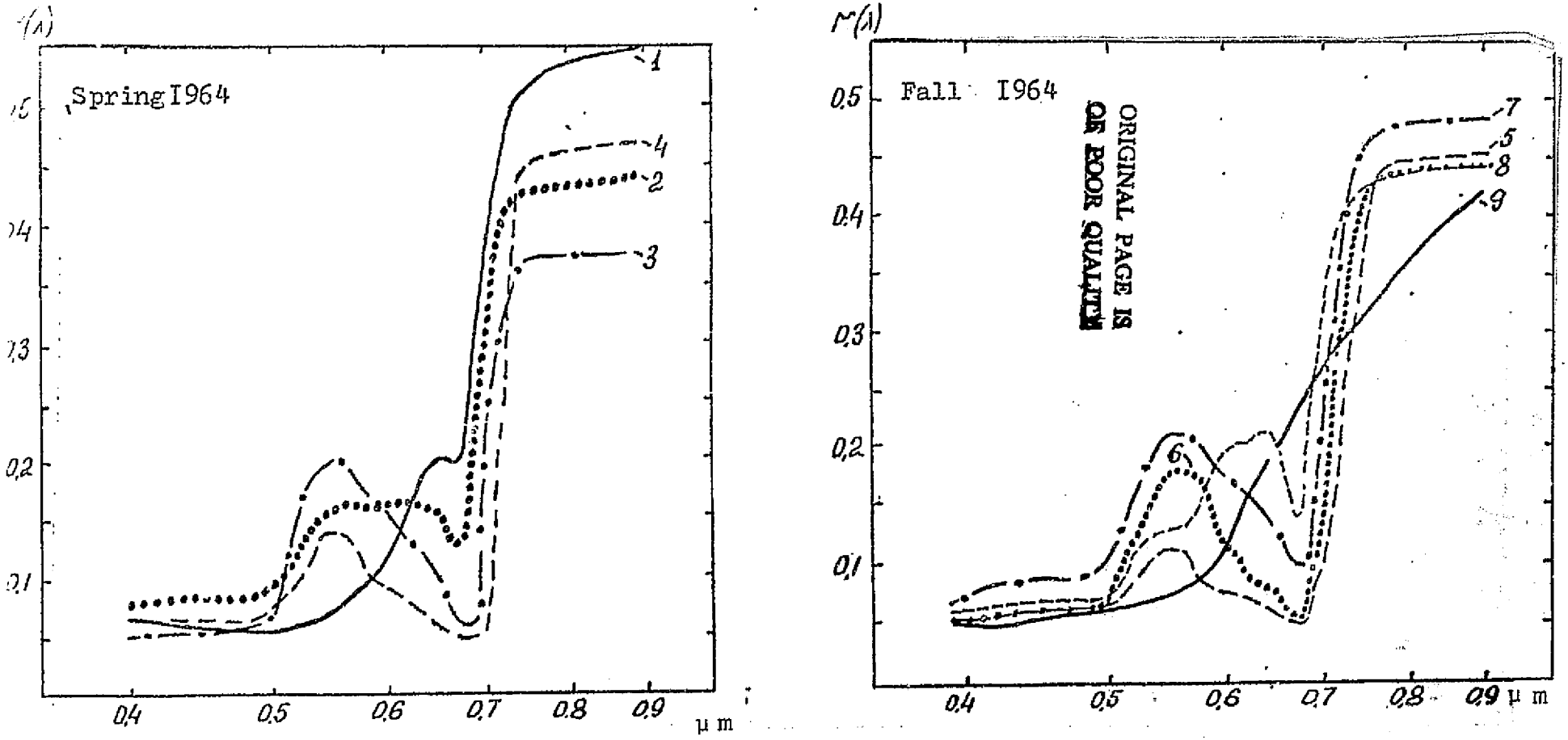

Fig. 21. [37] Spectral brilliance coefficients of oak leaves (Quercus alba): 1-April 17, 1964, 2-May 22, 1964, 3-May 5, 1964, 4-May 18, 1964, 5- September 18, 1964, 6-October 21, 1964, 7-October 26, 1964, 8-October 28, 1964, 9-November 2, 1964.

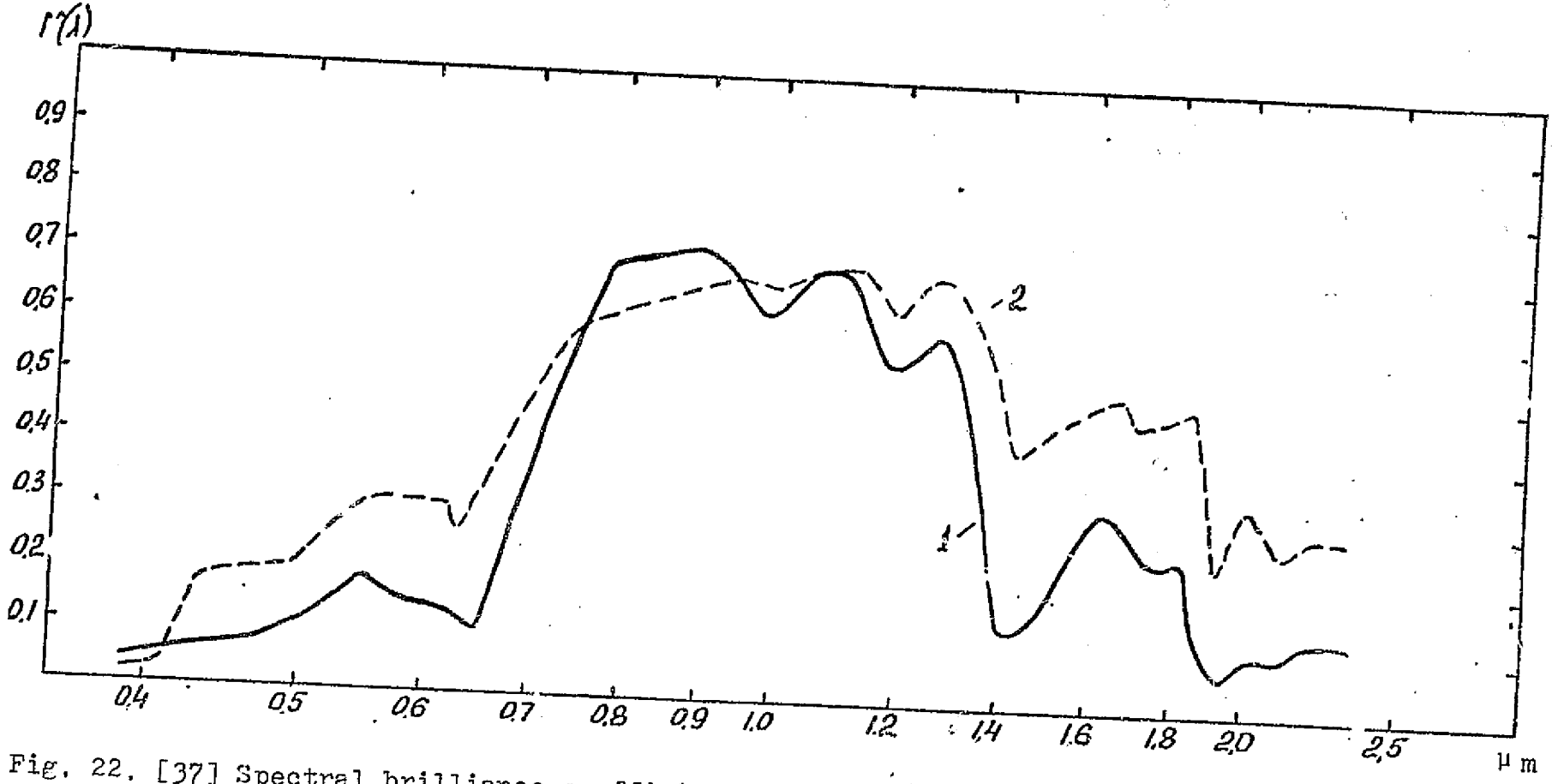

Fig. 22. [37] Spectral brilliance coefficients of pine (Ponferose Pine): 1-healthy; 2-diseased, dying.

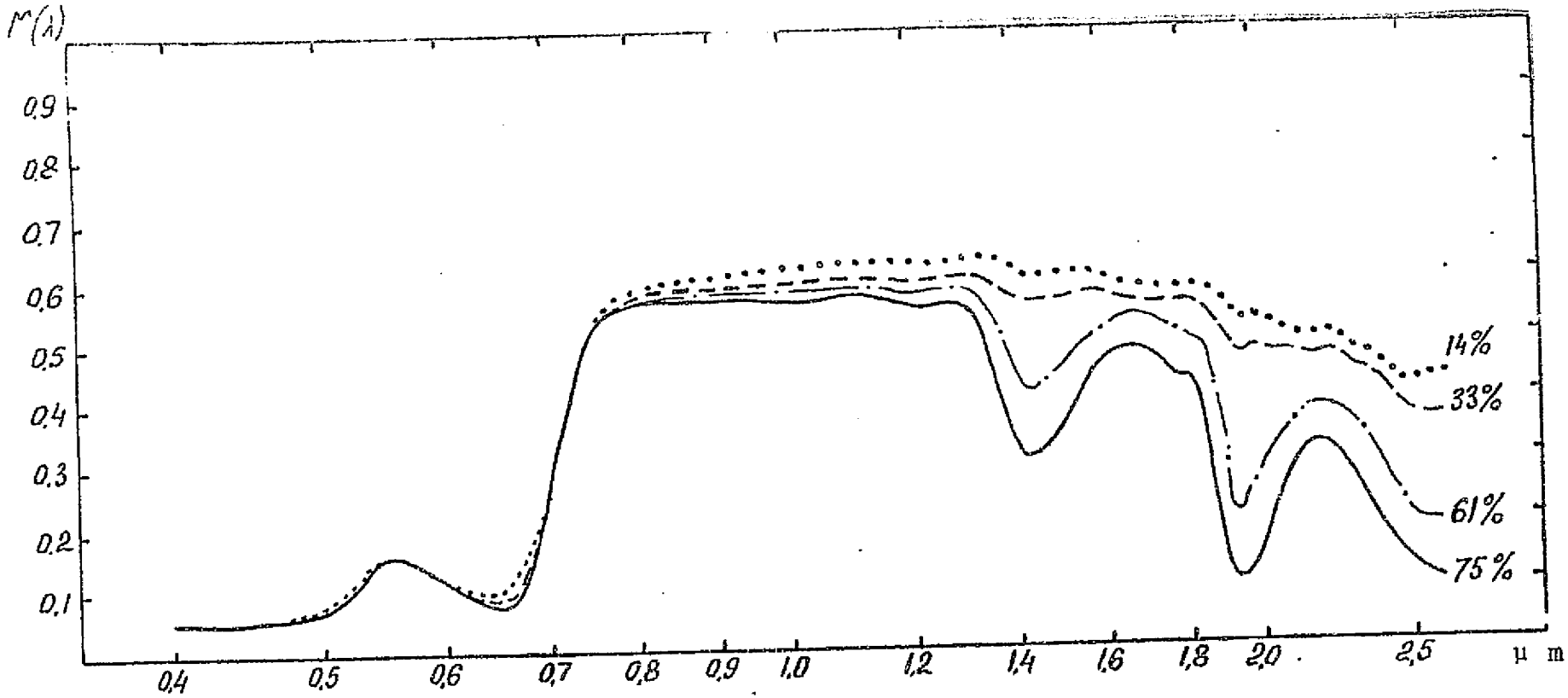

Fig. 23. [37] Spectral brilliance coefficients of leaves with various water contents.

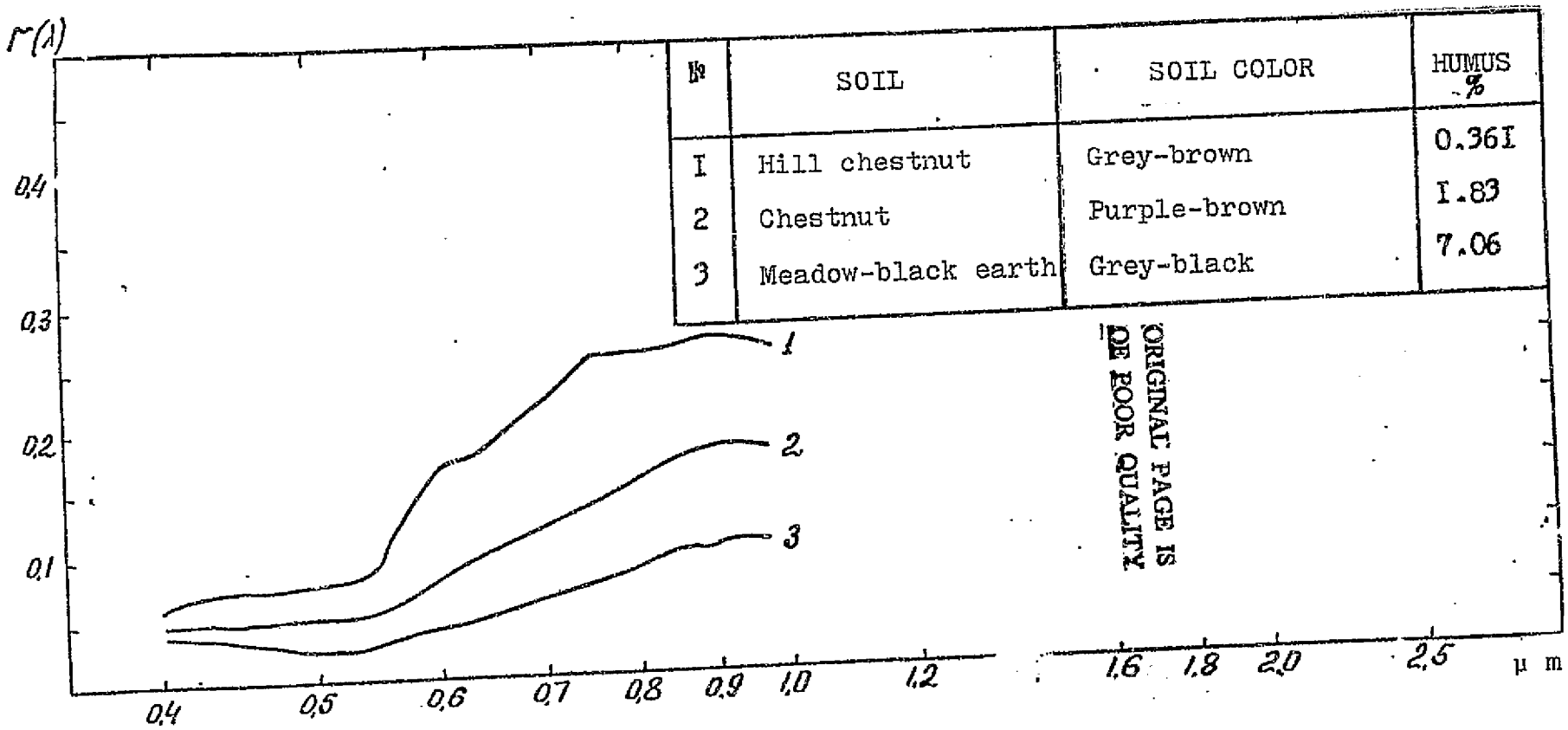

№	SOIL	SOIL COLOR	HUMUS %
I	Hill chestnut	Grey-brown	0.361
2	Chestnut	Purple-brown	1.83
3	Meadow-black earth	Grey-black	7.06

Fig. 24. [17] Spectral brilliance coefficients of various soils.

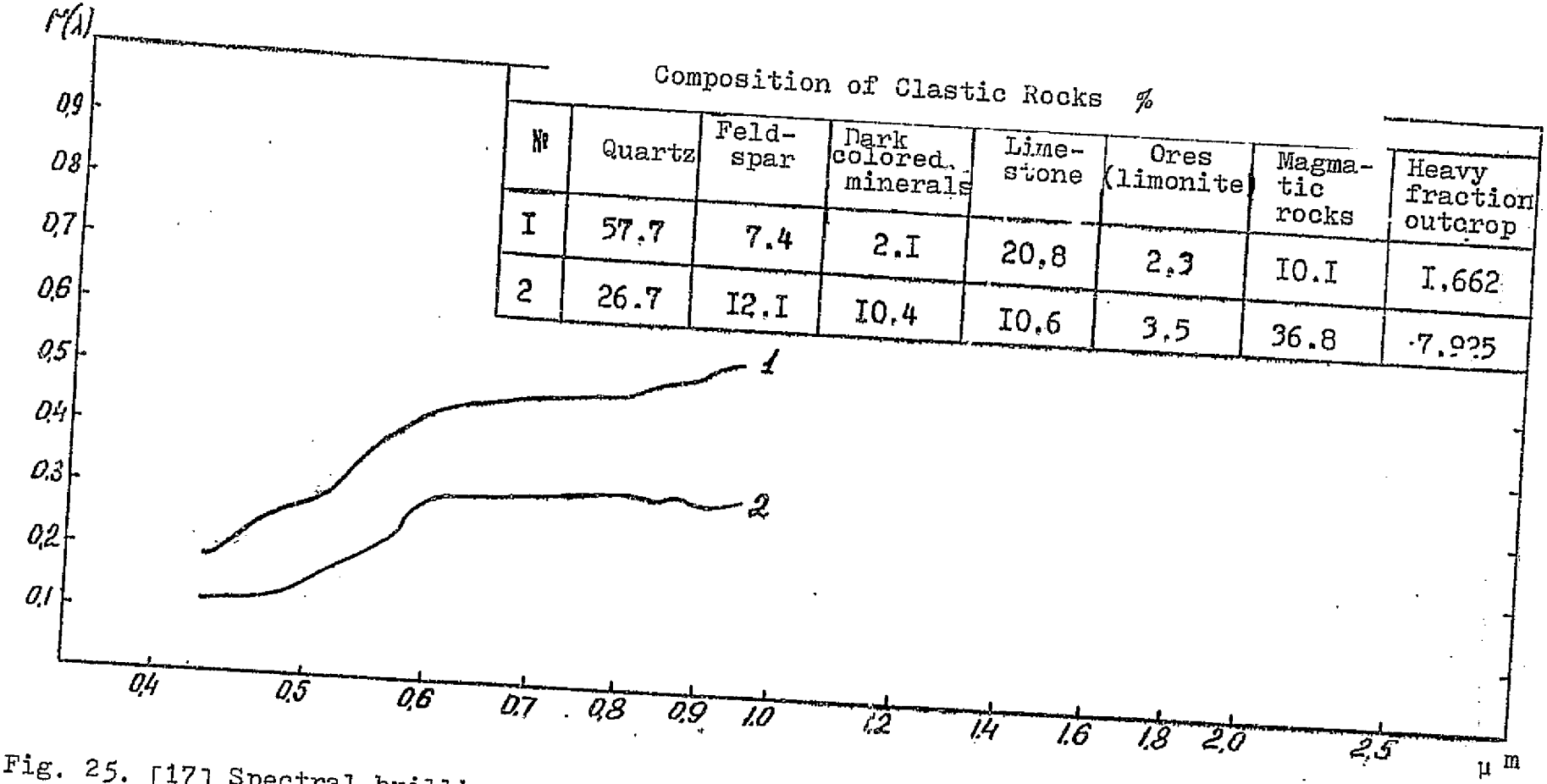

Composition of Clastic Rocks %

№	Quartz	Feld-spar	Dark colored minerals	Lime-stone	Ores (limonite)	Magma-tic rocks	Heavy fraction outcrop
I	57,7	7.4	2.I	20,8	2,3	I0.I	I,662
2	26.7	I2.I	I0.4	I0.6	3.5	36.8	7,925

Fig. 25. [17] Spectral brilliance coefficients of dry sub-gray-wacke (1) and gray-wacke (2) sands and their petrographic compositions.

Fig. 26. [17]Spectral brilliance coefficients of muddy loam at various moisture contents.

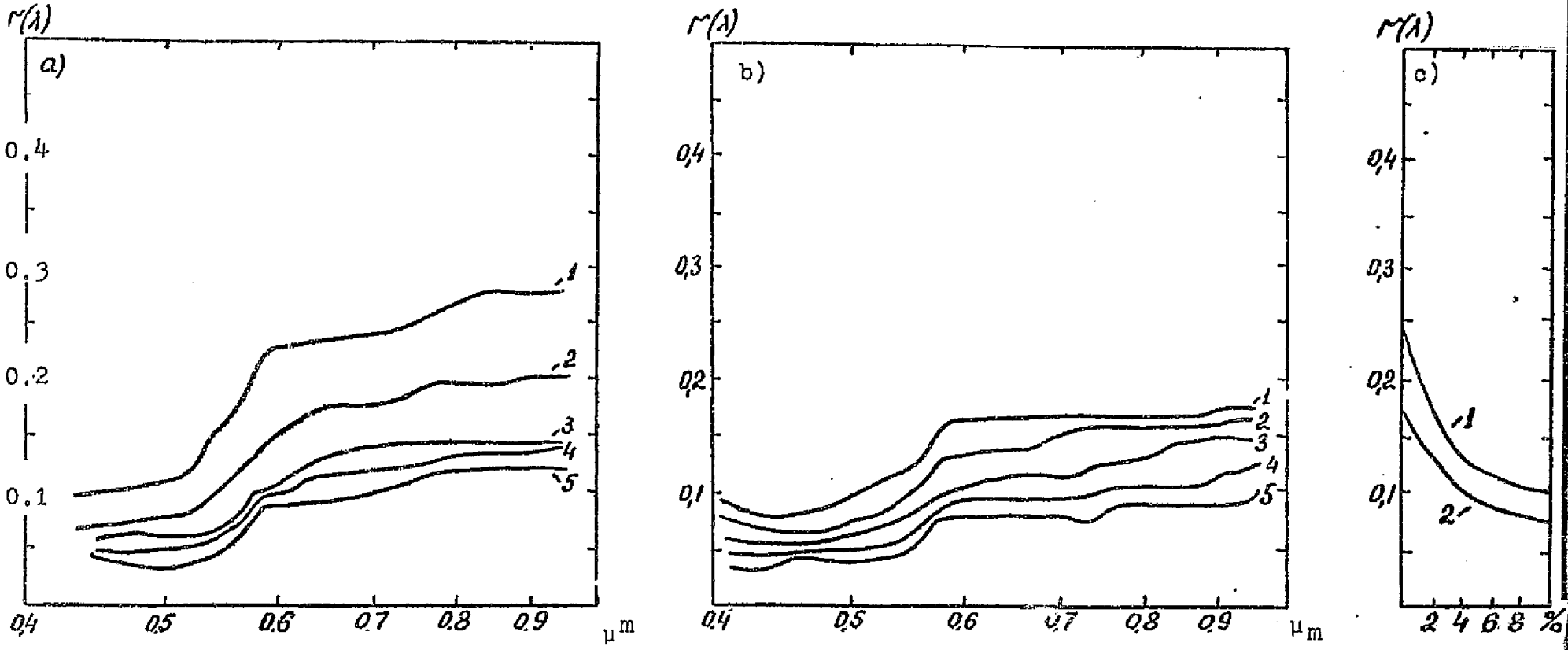

Fig. 27. [17] Spectral brilliance coefficients of sand with various moisture contents: a)-quartz, 1-dry, 2-2%, 3-3%, 4-5%; b) magnetite, 1-dry, 2-2%, 3-3%, 4-5%, 5-10%; c) the dependence of $r(\lambda)$ of quartz (1) and magnetite (2) sand on moisture content for $\lambda = 0.7$ μm.

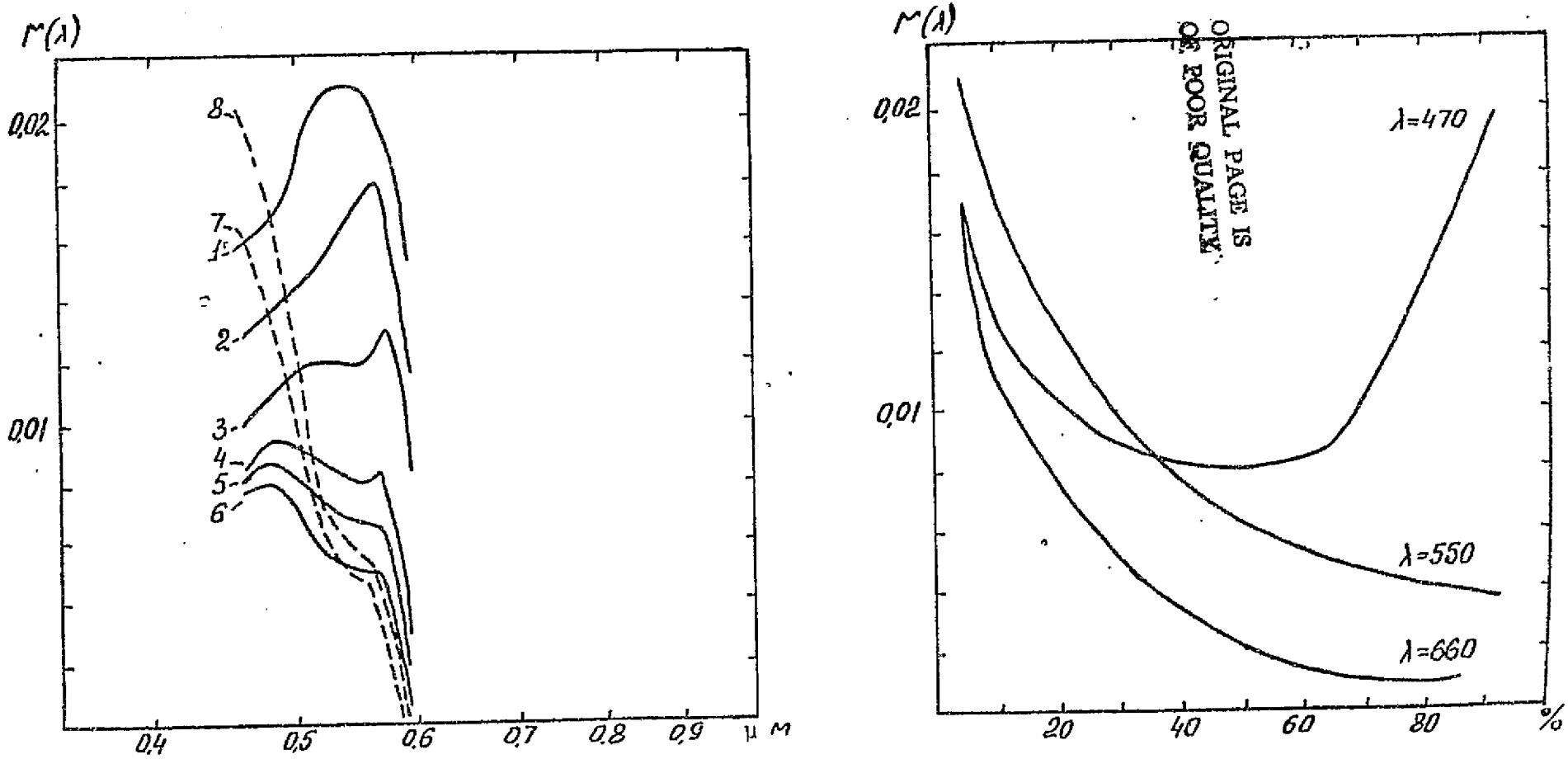

Fig. 28. [25] Spectral brilliance coefficients for sea surfaces of varying transmittance t' for the water: a) course of $\Gamma(\lambda)$ at different t': 1-5%, 2-10%, 3-27%, 4-38%, 5-59%, 6-69%, 7-84%, 8-86%; b)the dependence of $\Gamma(\lambda)$ on the transmittance of the water t' for three spectral intervals.

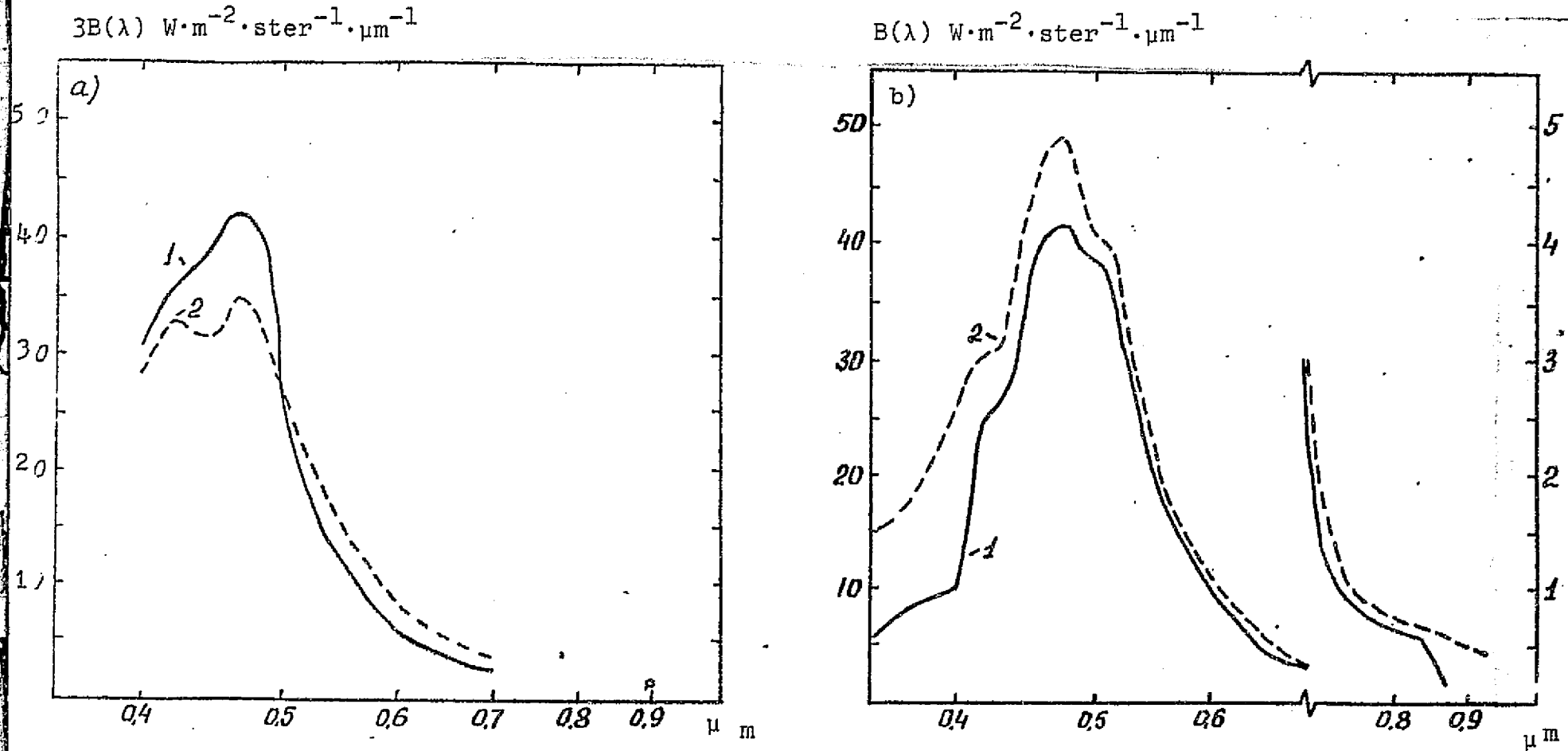

Fig. 29. Spectral brilliances of the surface of the ocean, a) [39] with chlorophyll concentration: 1-0.0..., 2-0.2 mg/m^3; b) [42] 1-clean surface; 2-surface covered with petroleum film.

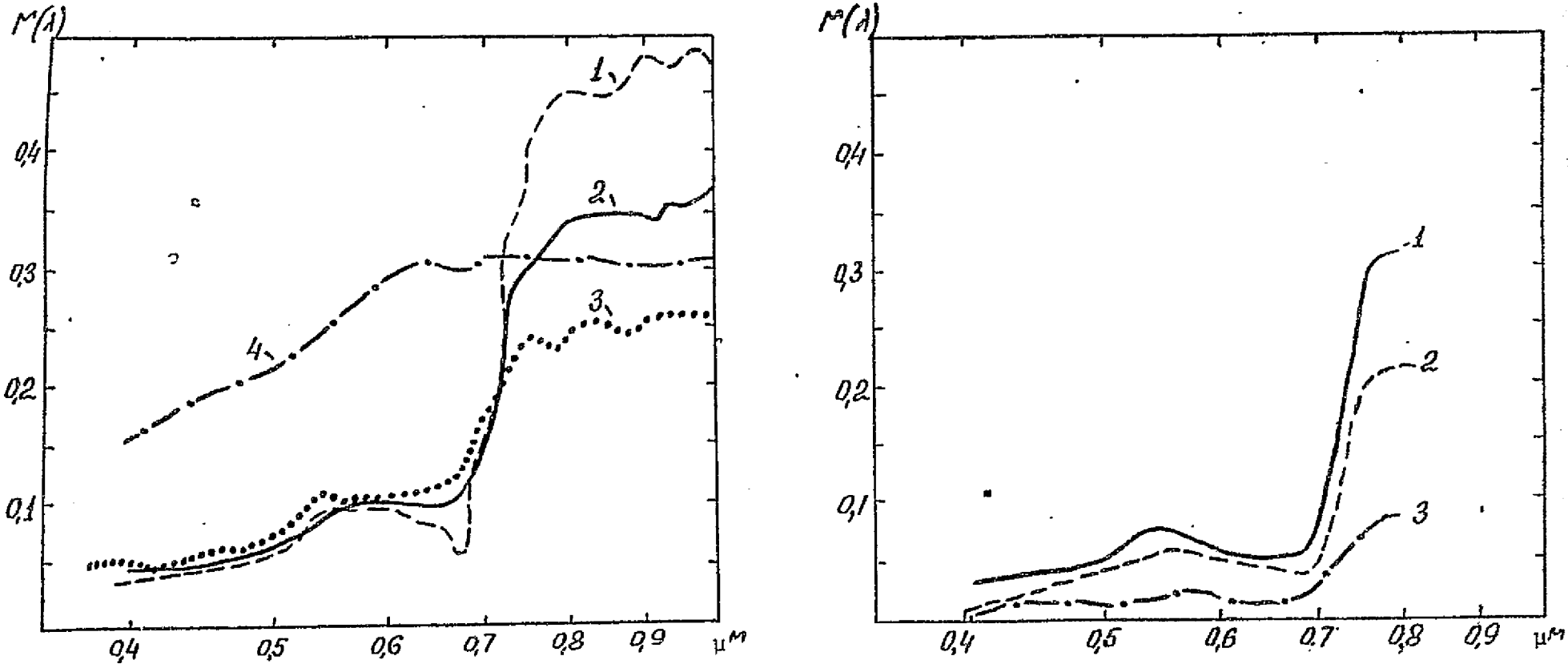

Fig. 30. Spectral brilliance coefficients a) [17] wormwood in budding stages on a rocky talus with various areas of projected covering: 1- S_n=100%, 2-S_n=80%, 3-S_n =50%, 4-S_n =0; b) 18 pine with crowns of various thicknesses: 1-100%, 2-80%, 3-50%.

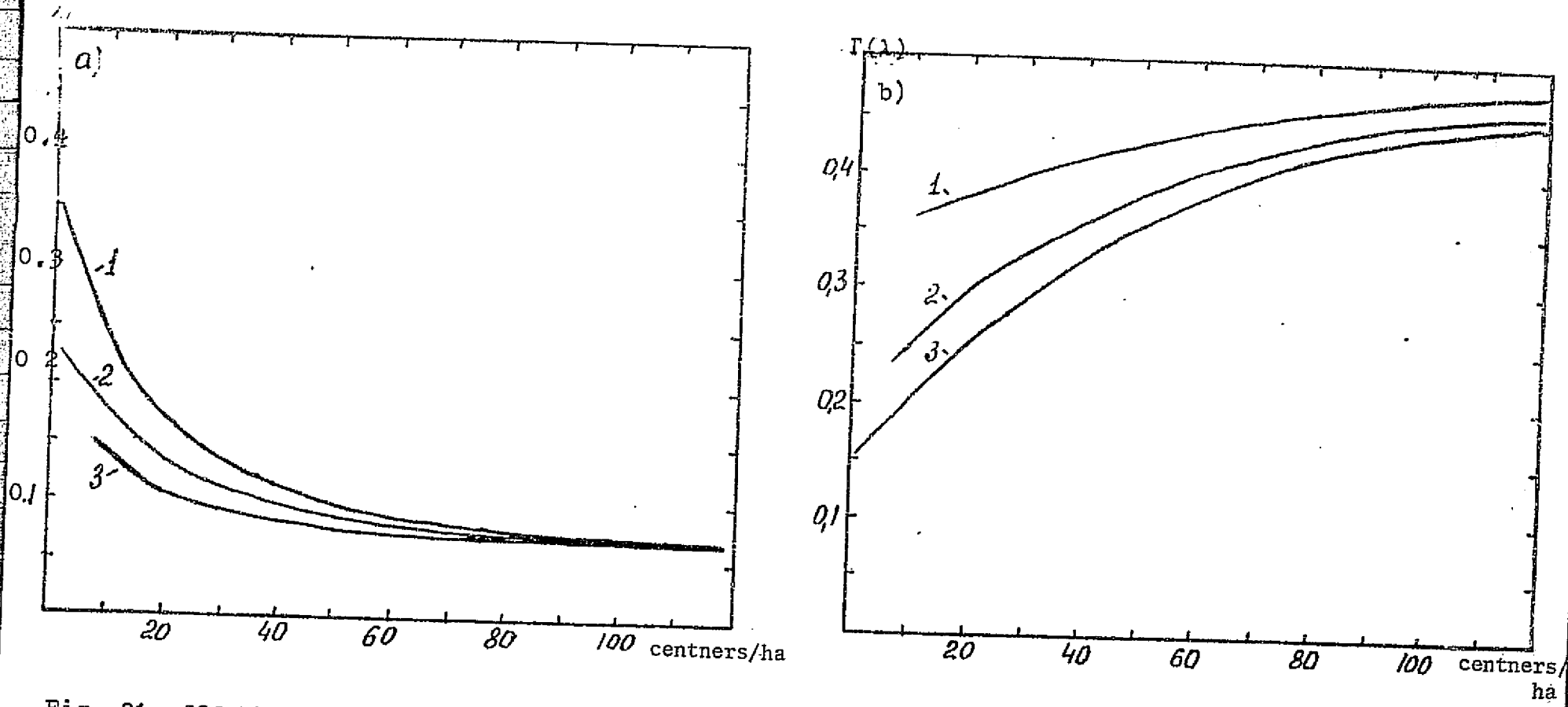

Fig. 31. [9] The relation between the brilliance coefficients of soil-plant covering systems and the quantity of green mass for various types of soil in the spectral intervals 0.59÷0.72 μm (a) and 0.68÷1.2 μm (b).
I- clay soil, 2-light sand, 3-dark sand

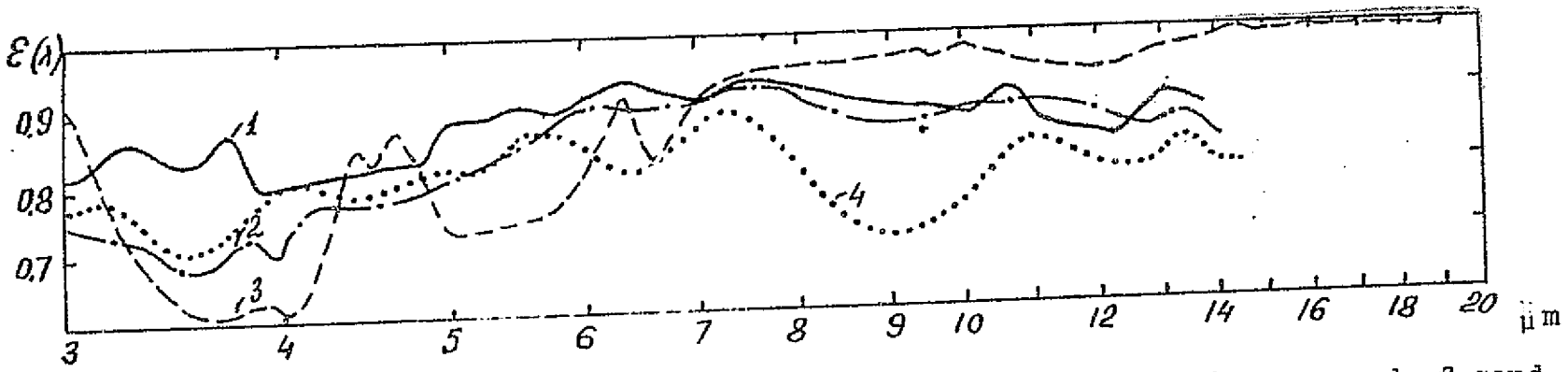

Fig. 32. Spectral radiation coefficients: 1-clay, 263 K [2]; 2- soil composed of sand, clay, and dark-grey flagstone, 263 K [2]; 3- dry clay soil [34]; 4-small pebbles, 263 K [2].

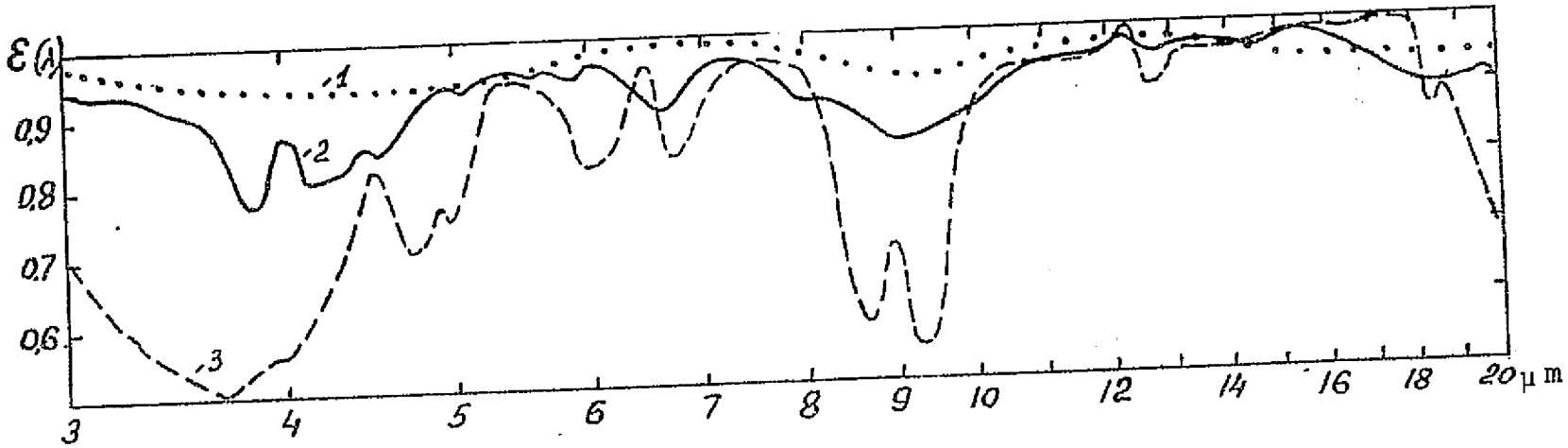

Fig. 33. Spectral radiation coefficients: 1- asphalt [19]; 2-red sandstone [36]; 3-sandy beach [34].

Classification names of rocks	Ultrabasic	Basic	Intermediate	Acidic
Concentration	less than 45%	45÷53%	53÷65%	greater than 65%
Example	dunite	basalt	syenite	granite

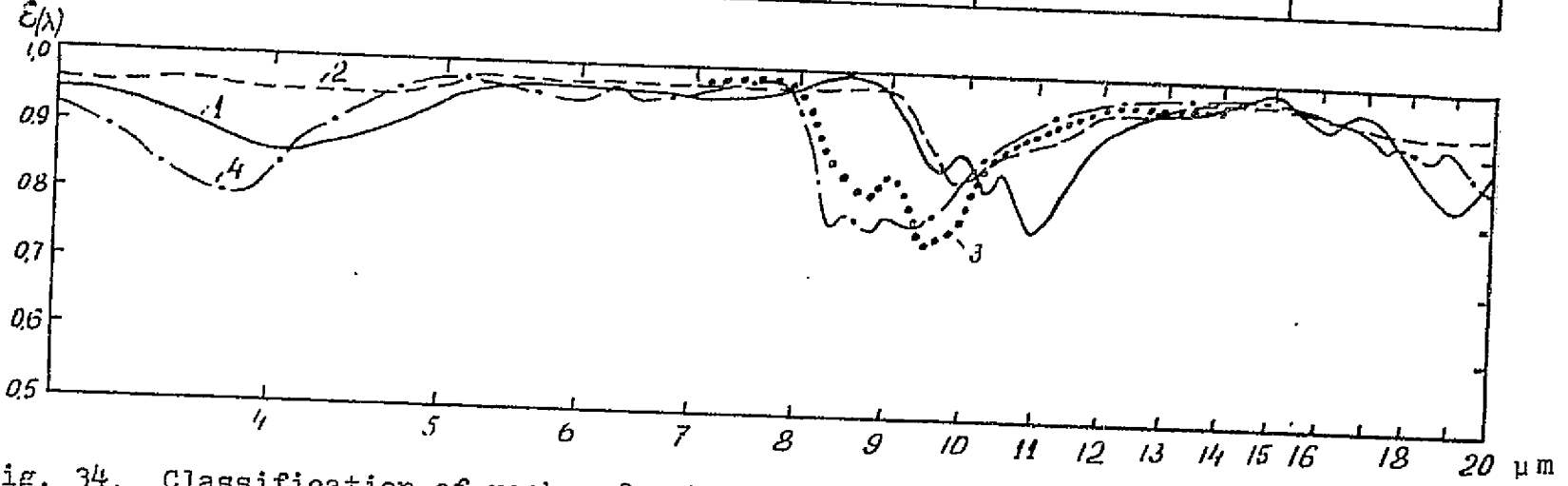

Fig. 34. Classification of rocks of volcanic origin [36] and spectral radiation coefficients of samples of them: 1-dunite [36]; 2-basalt [36]; 3-pyroxene syenite [41]; 4-granite [36].

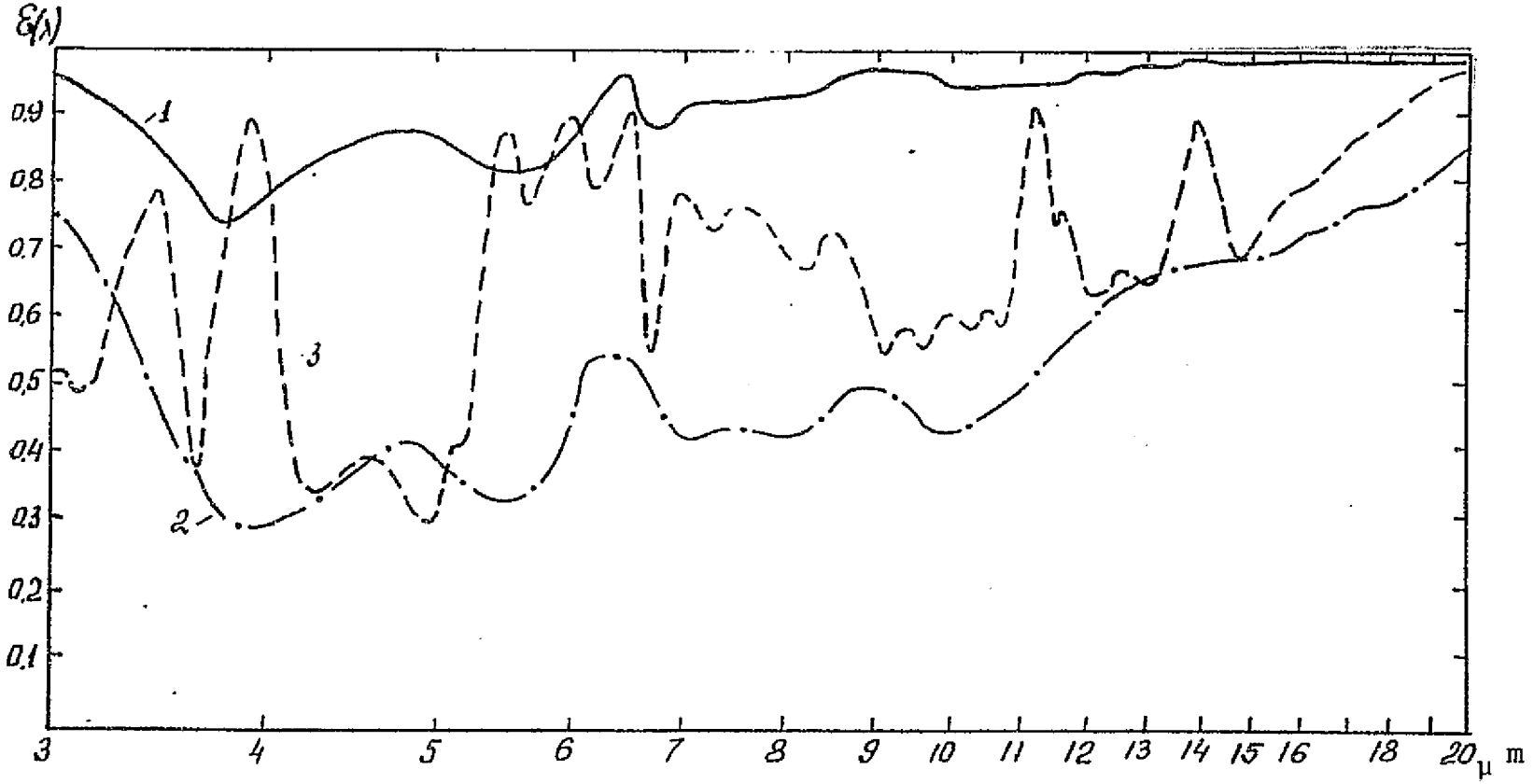

Fig. 35. Spectral radiation coefficients: 1-saline reservoir [34]; 2-NaCl [34]; 3-$CaCO_3$ [34].

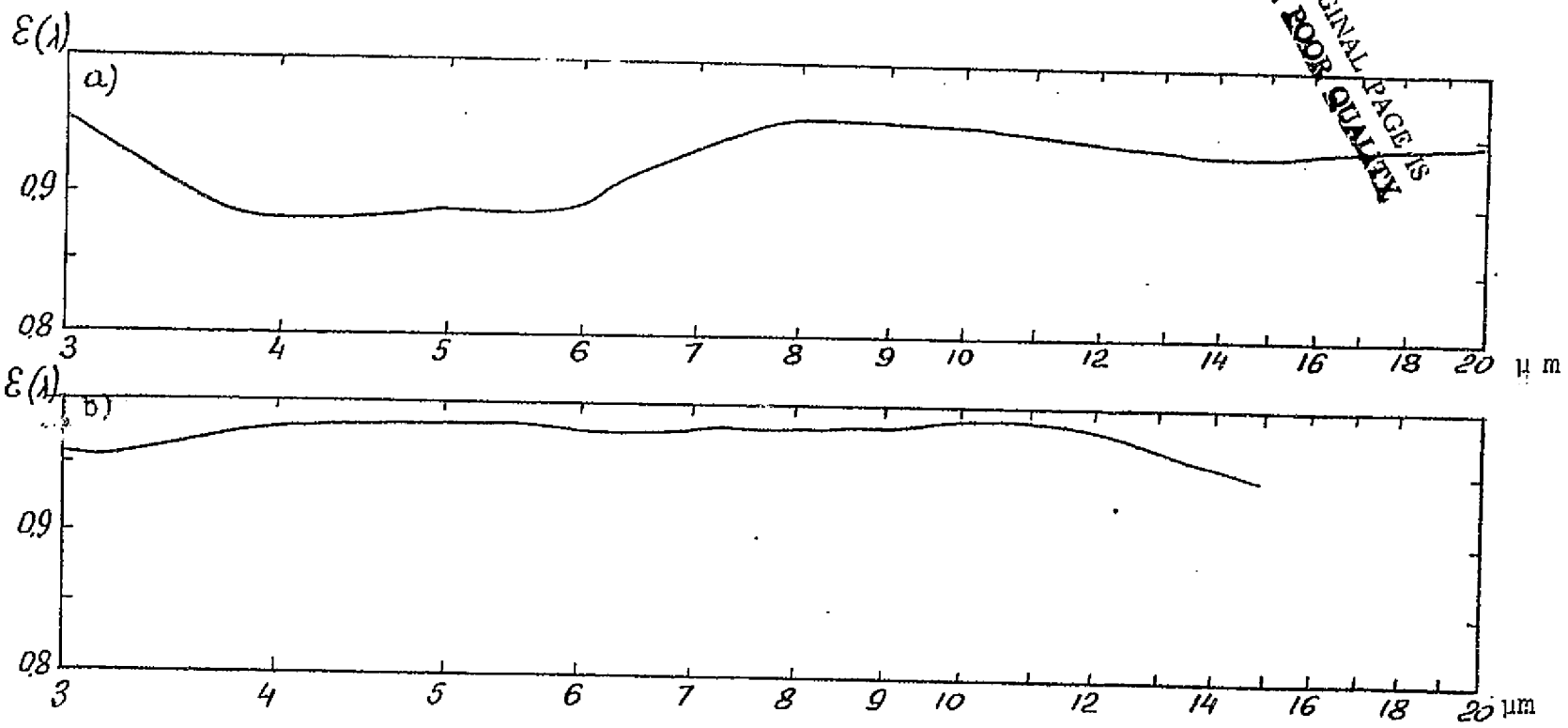

Fig. 36. Spectral radiation coefficients: a)-green leaf of an indoor lemon [19]; b)-water (θ=0) [2].

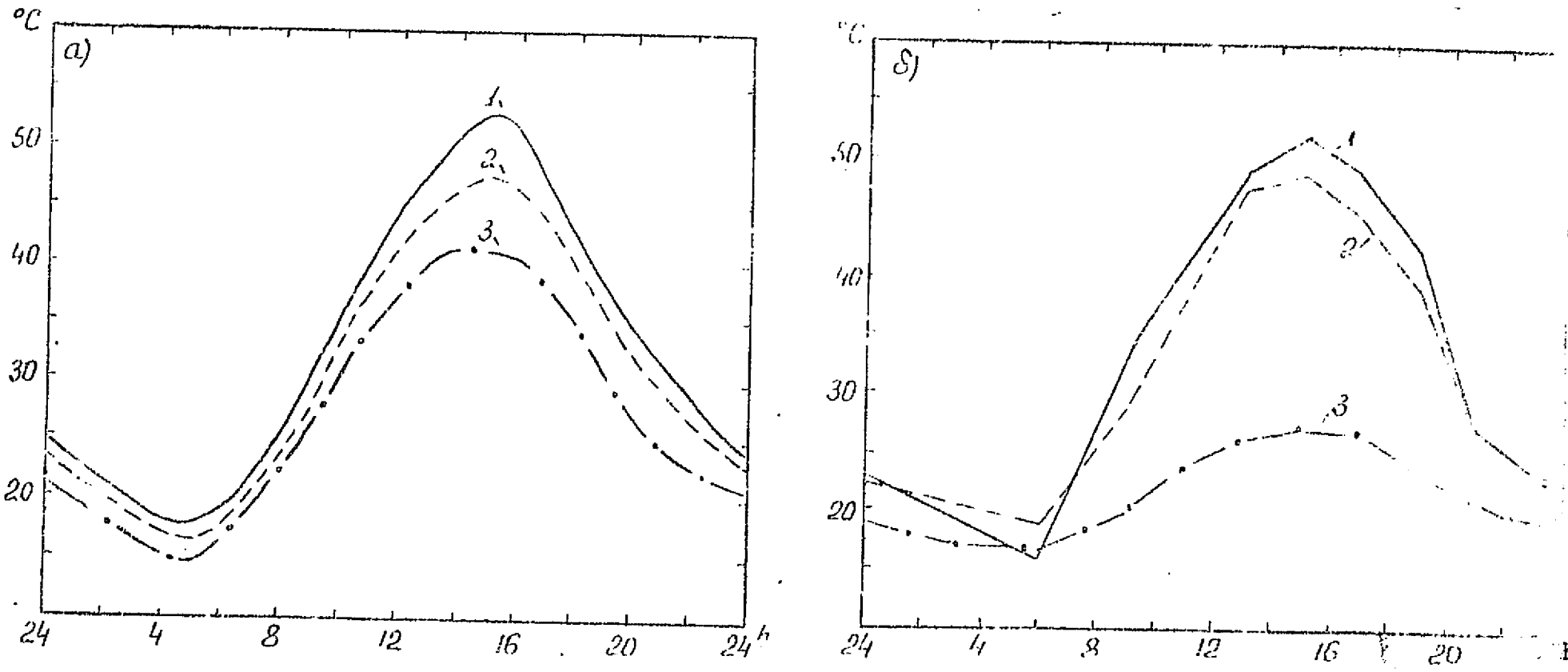

Fig. 37. Daily course of temperature: a) on road surfaces on a cloudless summer day [37]; 1-3" asphalt layer; 2-packed sandy soil; 3-9" concrete layer; b) [3] 1-on a dirt road; 2-on a wormwood plain; 3-in a damp hollow with thick meadow vegetation.

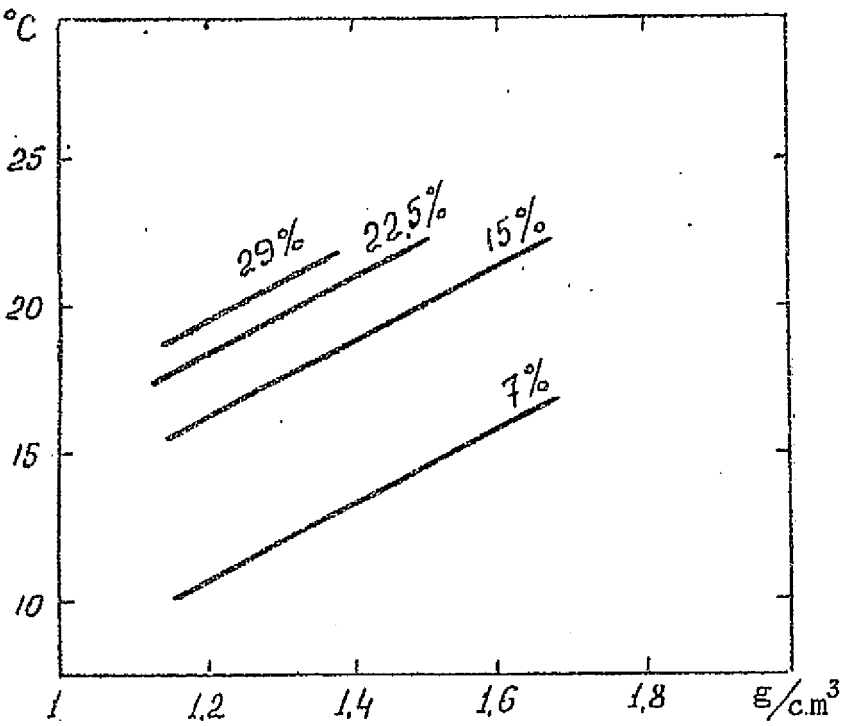

Fig. 38. [37] The dependence of the temperature of a clay soil surface on its density and moisture content (at 5:00 A.M. on a cloudless summer morning).

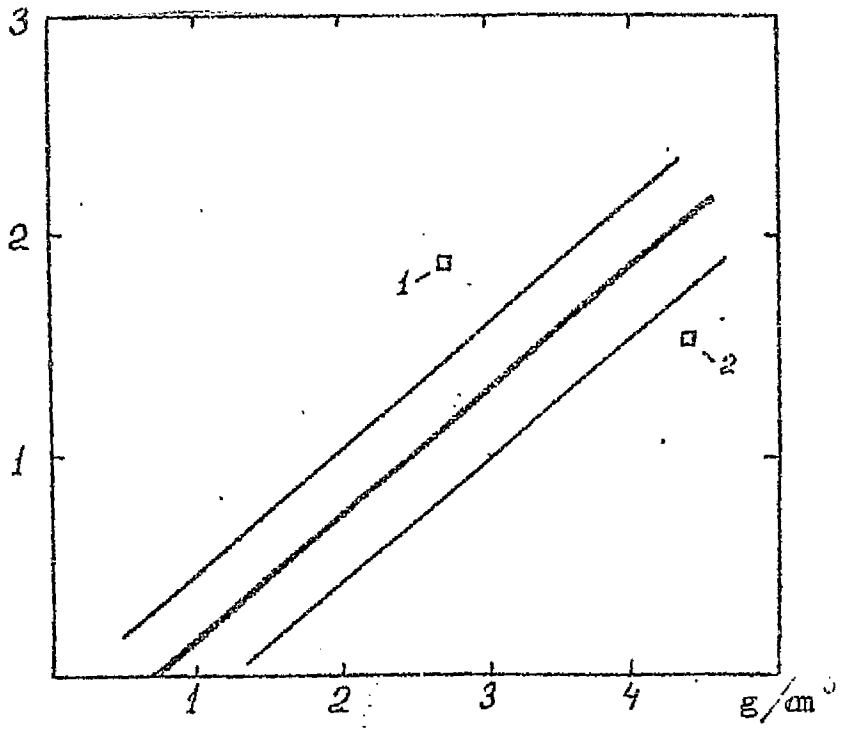

Fig. 39. [43] The dependence of thermal inertia (relative unit) on density for various rock-forming minerals, rocks and soils. A direct linear correlation exists between the lines, conforming to standard deviations. Specific characteristic thermal inertia values of quartz (1) and olivine (2).

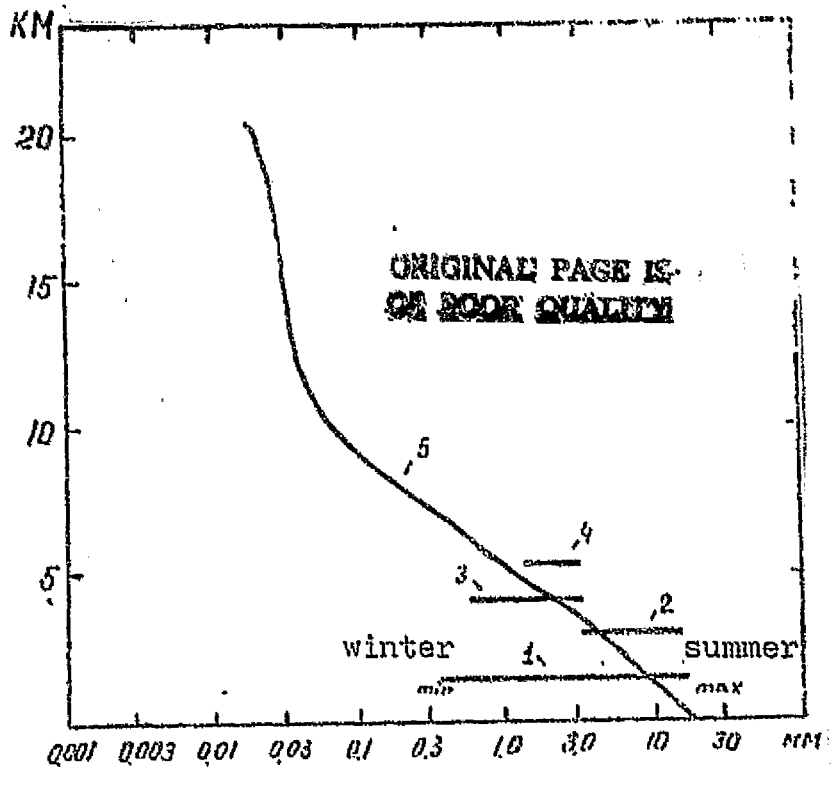

Fig. 40. [24]
The water vapor concentration in the earth's atmosphere in a vertical path in mm from precipitated water at a given altitude: 1-Denver, USA; 2-El'brus, USSR; 3-Evans, USA; (summer): 4-Chakartaya, Bolivia; 5-average global data.

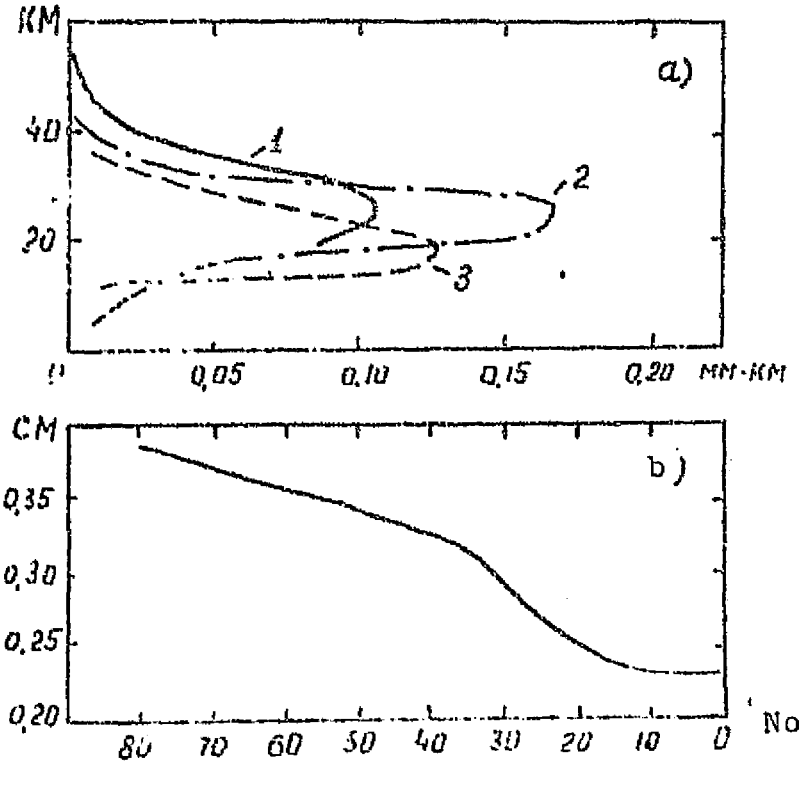

Fig. 41.
Ozone concentration in the earth's atmosphere: a) the amount of ozone in a vertical path in mm in 1km at a given altitude [24]: 1-June; 2-October; 3-April.

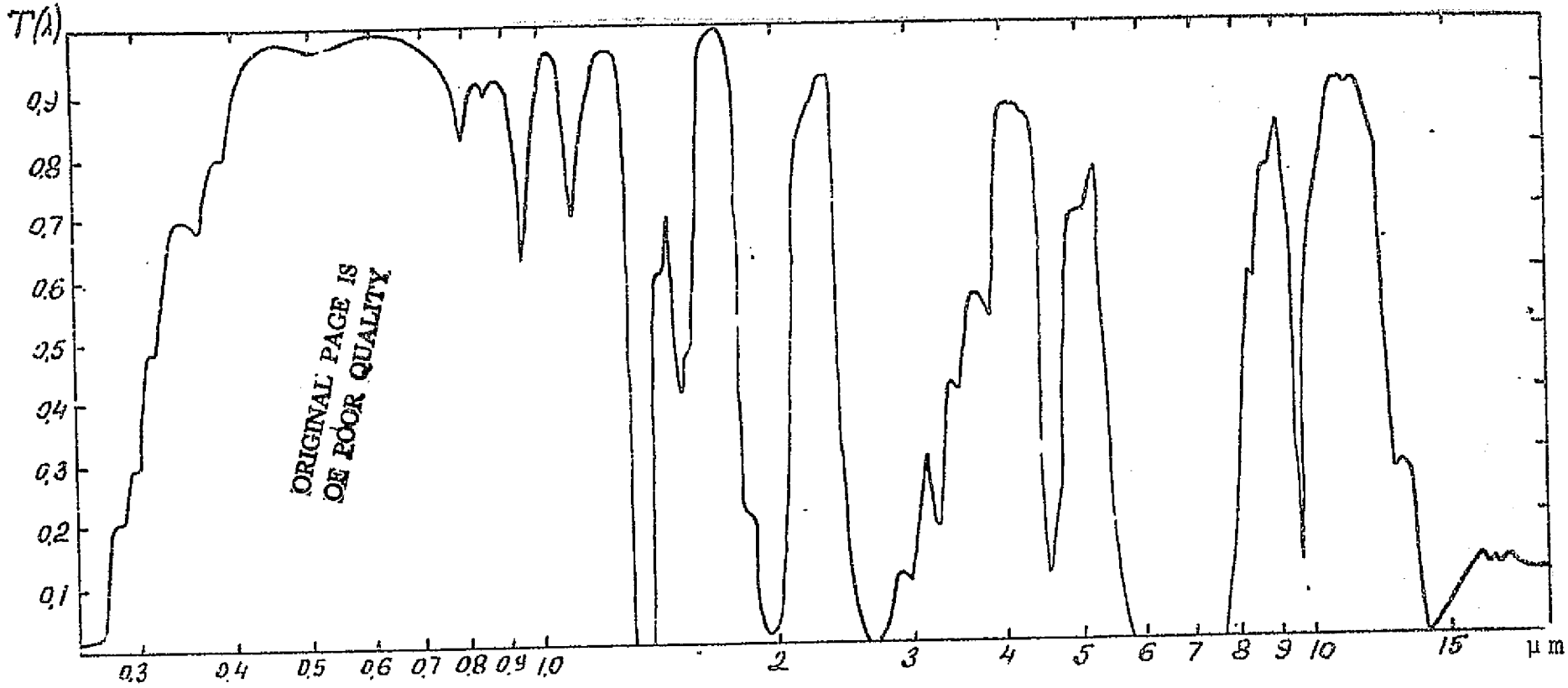

Fig. 42. [44] Spectral transmission in the earth's atmosphere on a vertical course.

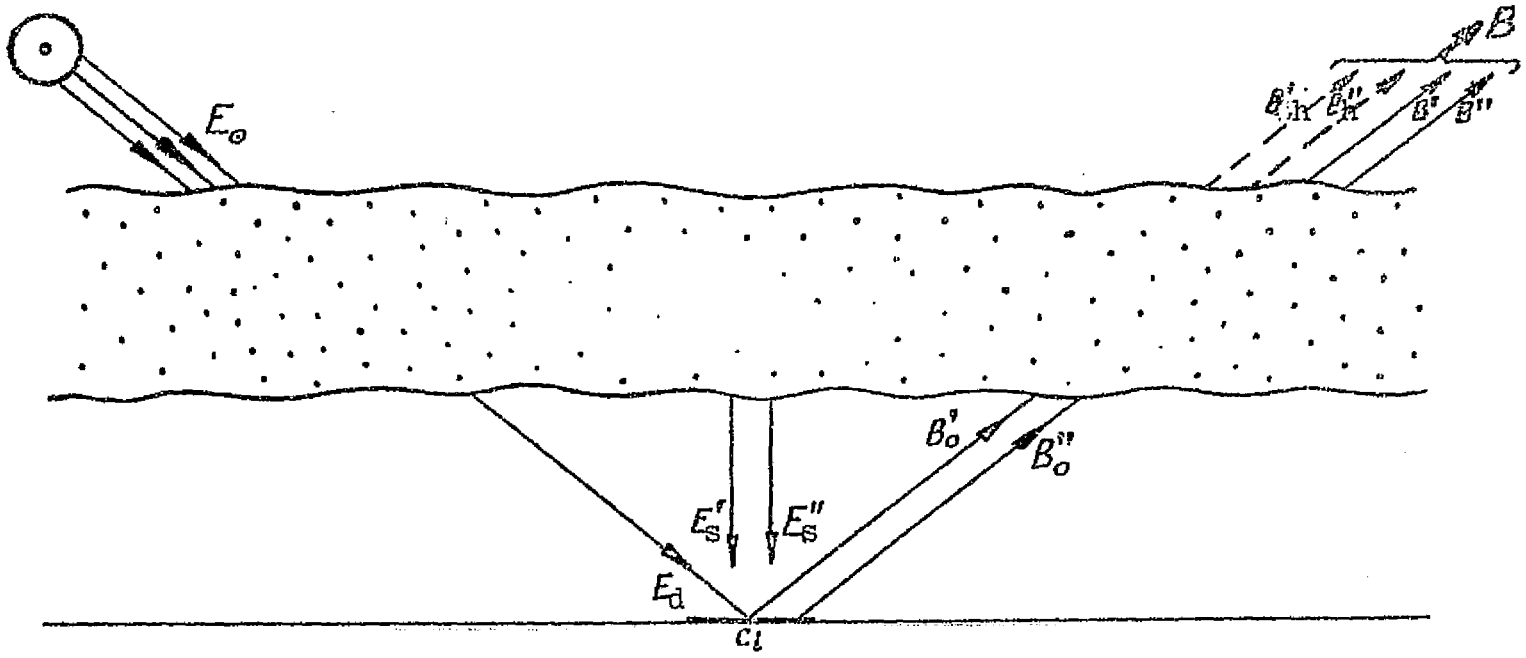

Fig. 43. Transfer of radiation currents in the earth's atmosphere.
$E_\odot$-density of solar radiation on the upper limit of the earth's atmosphere;
E_d, E'_s, E''_s-irradiation of object c_i direct and scattered solar radiation and thermal back radiation in the atmosphere;
B'_o and B''_o- brilliance of object c_i due to reflected solar radiation and inherent radiation;
B-remote measurement (observed) of the brilliance of object c_i;
B' and B"- basic components of remote measurements of brilliance B, coming from object c_i in reflected and inherent radiation; B'_h- atmospheric haze brilliance caused by scattering; B''_h- brilliance of inherent radiation in the atmosphere.

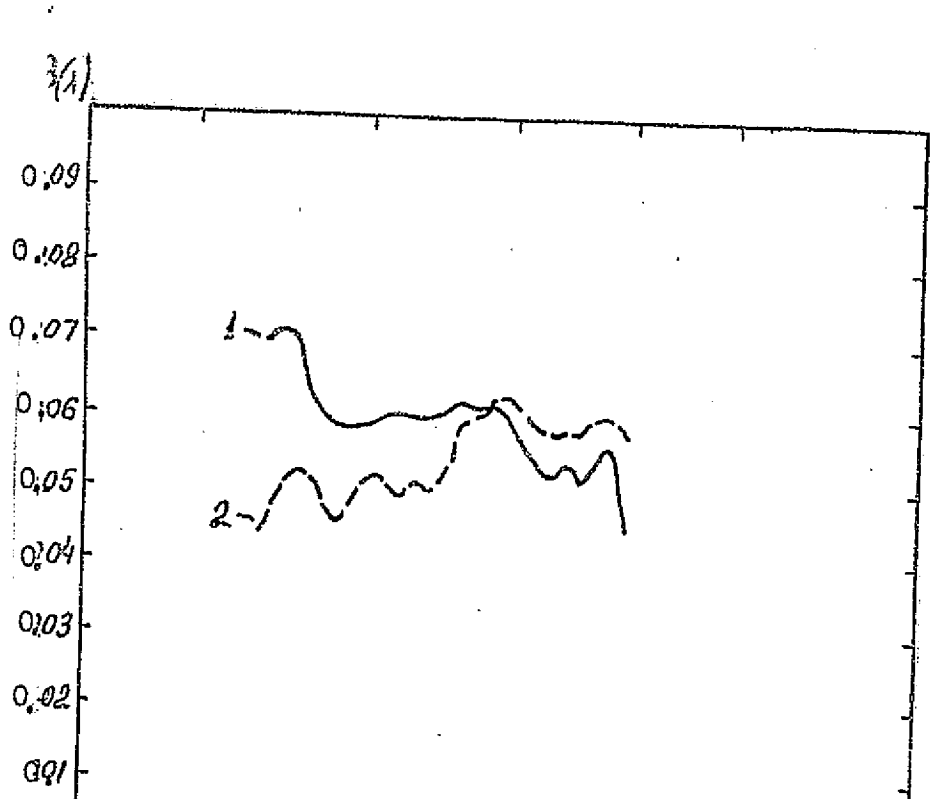

Fig. 44. [9] Spectral brilliances of an underlying surface (on the shore of the Caspian Sea), measured on October 13, 1969: 1- with pilot channel receiver "Soyuz-7"; 2- with airplane LI-2

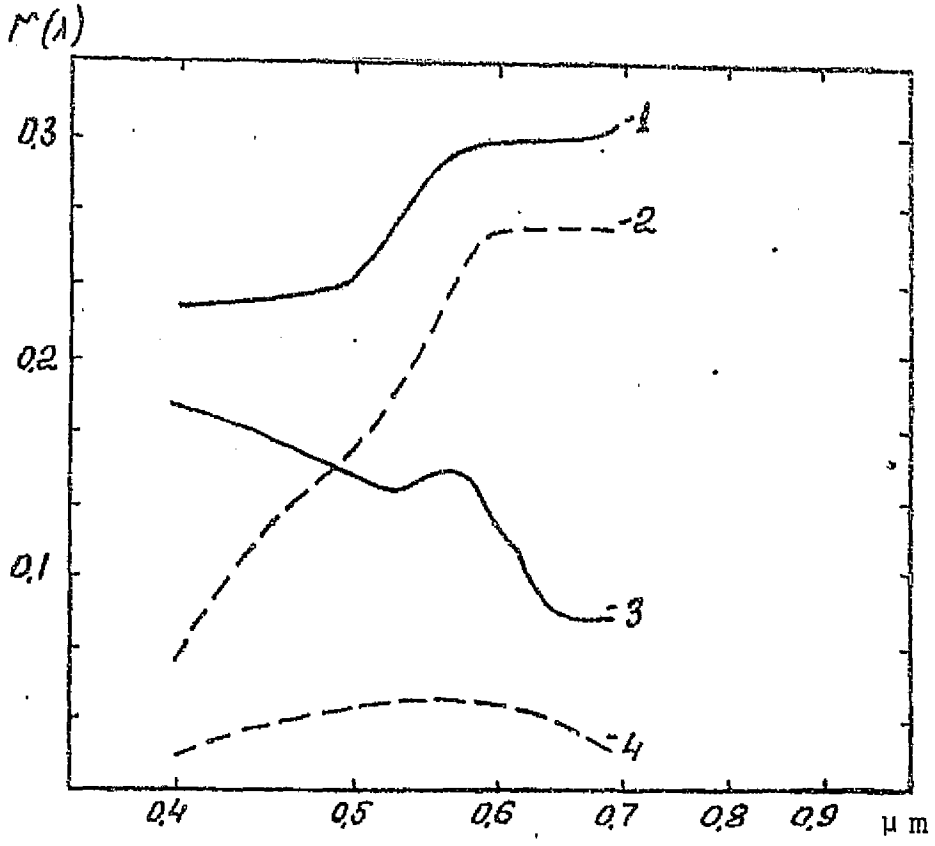

Fig. 45. [9] Spectral brilliance coefficients for two types of underlying surfaces, measured from space and from the surface of the earth: 1-sand, H=250 km; 2-sand, H=0; 3-water, H=250 km; 4-water H=0.

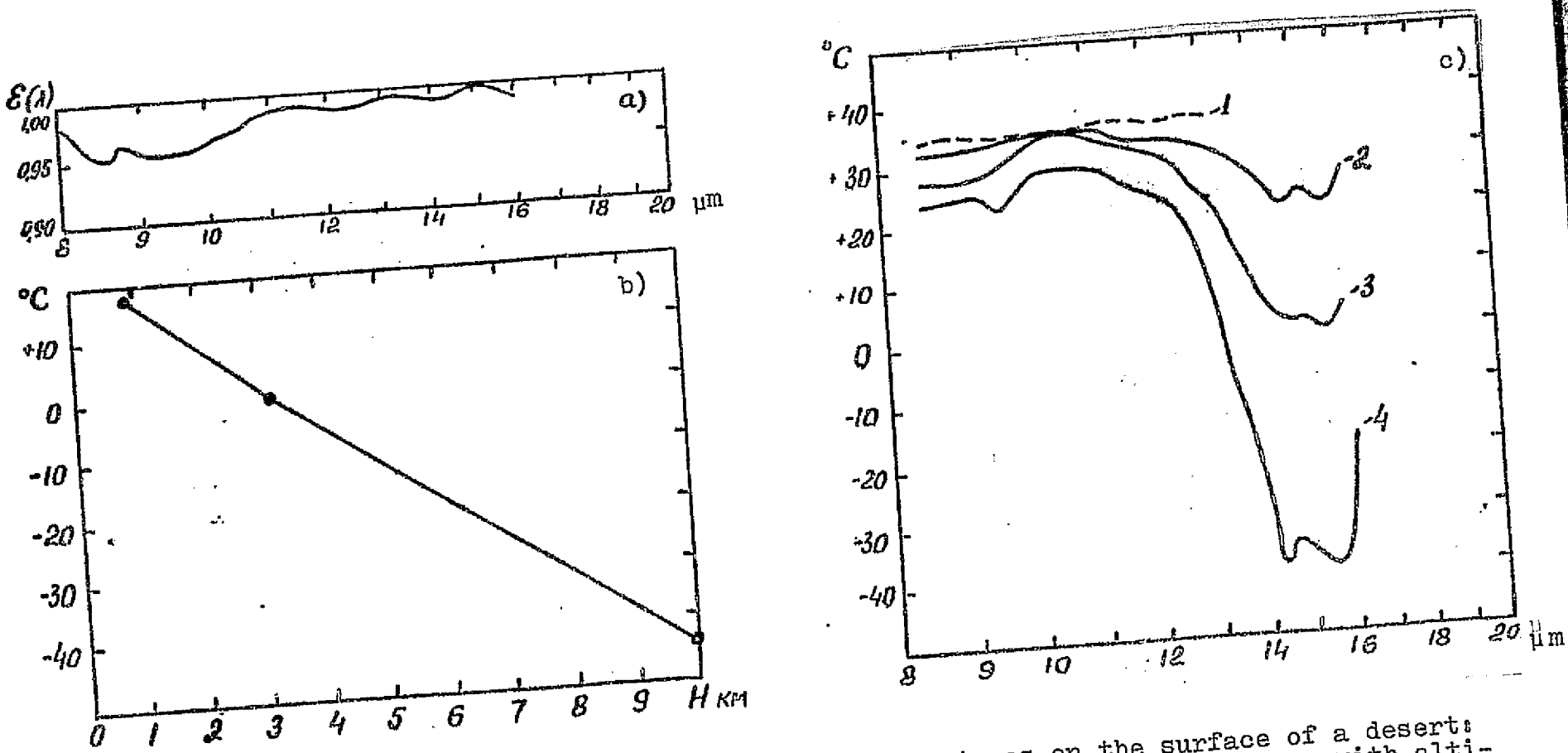

Fig, 46. [35] Spectral distribution of brilliance temperatures on the surface of a desert: a) radiation coefficient of the surface; b) change in air temperature with altitude; c) brilliance temperature values: 1-calculations of surface temperature 36 C without considering atmospheric influences; 2-measurements from an altitude of 0.91 km; 3-measurements from an altitude of 3.2 km; 4-measurements from an altitude of 10.05 km.

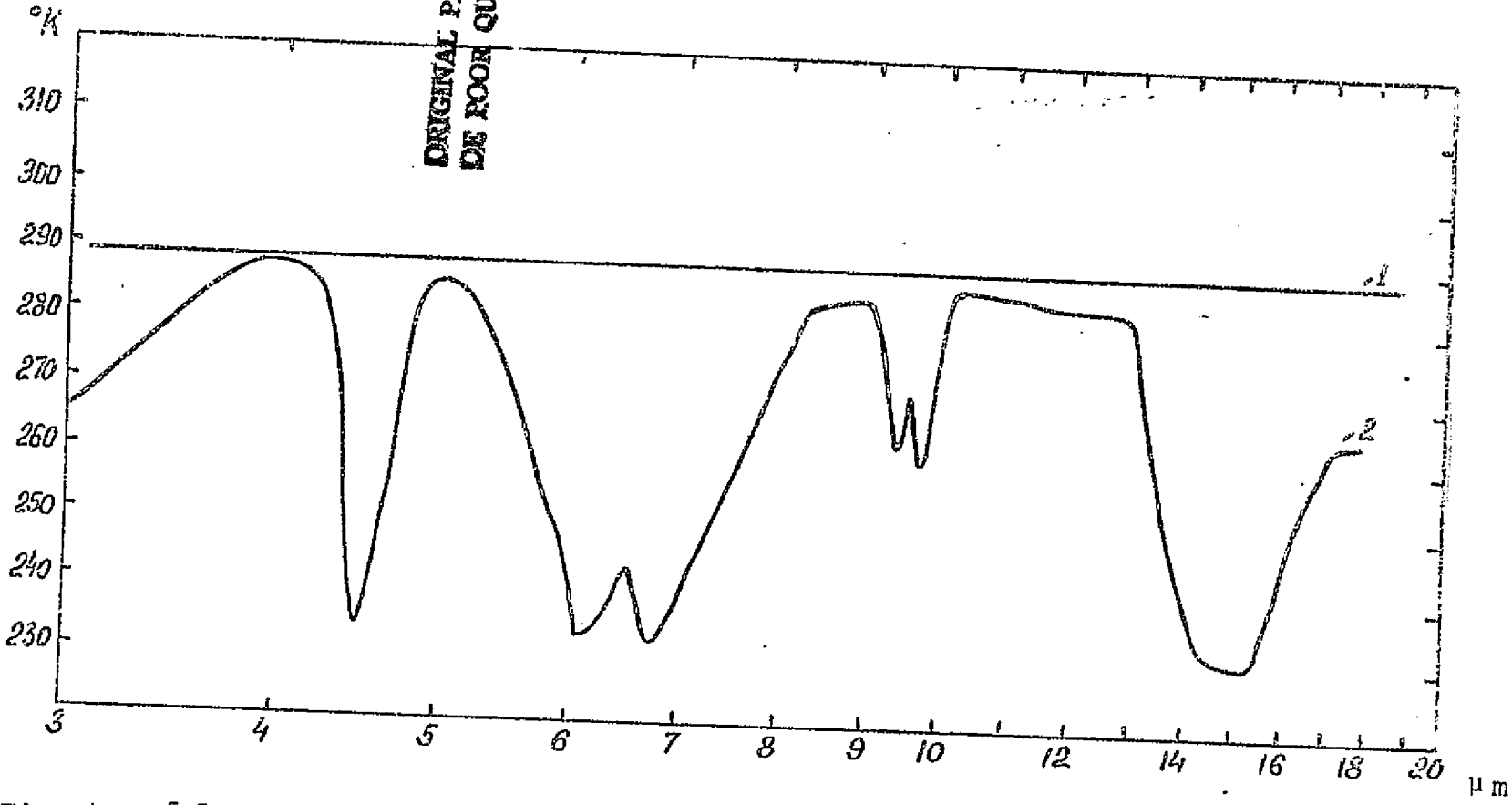

Fig. 47. [6]Spectral distribution of brilliance temperature values of an underlying surface, Leningrad, July: 1-true temperature; 2-radiative temperature.

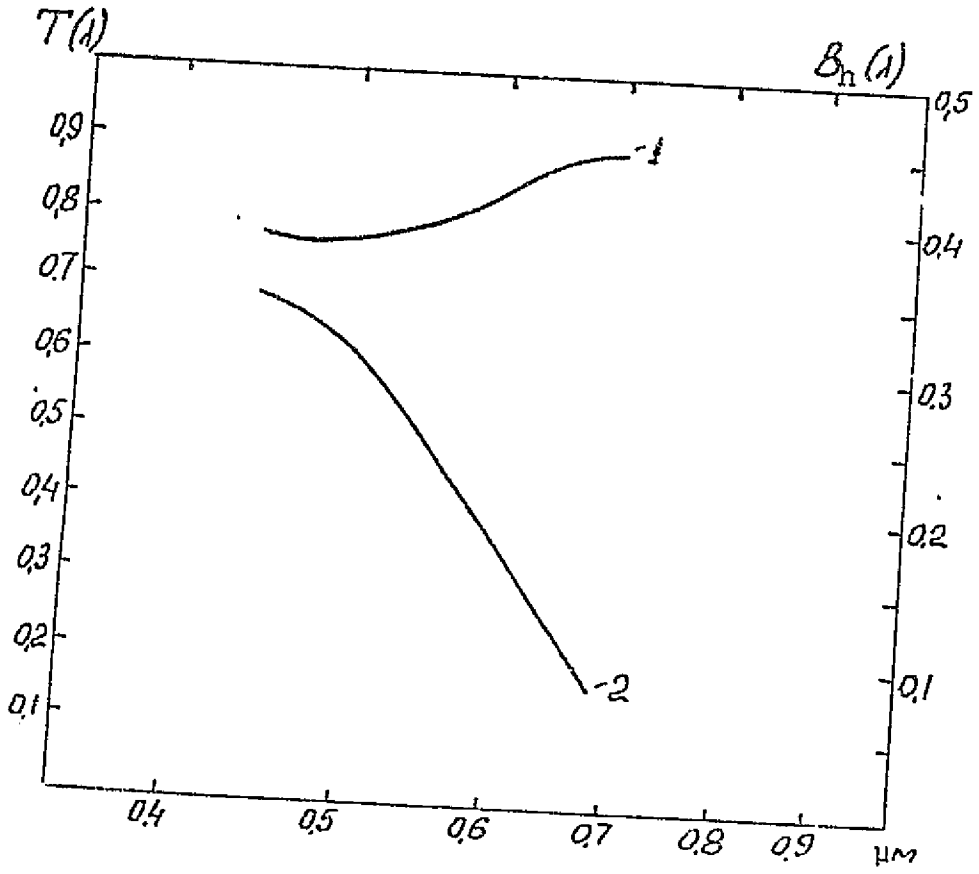

Fig. 48. [9] Spectral dependence of components of the atmospheric transmission function according to data from pilot channel receiver "Soyuz-7": 1-transmission radiation of the atmosphere; 2-brilliance of atmospheric haze.

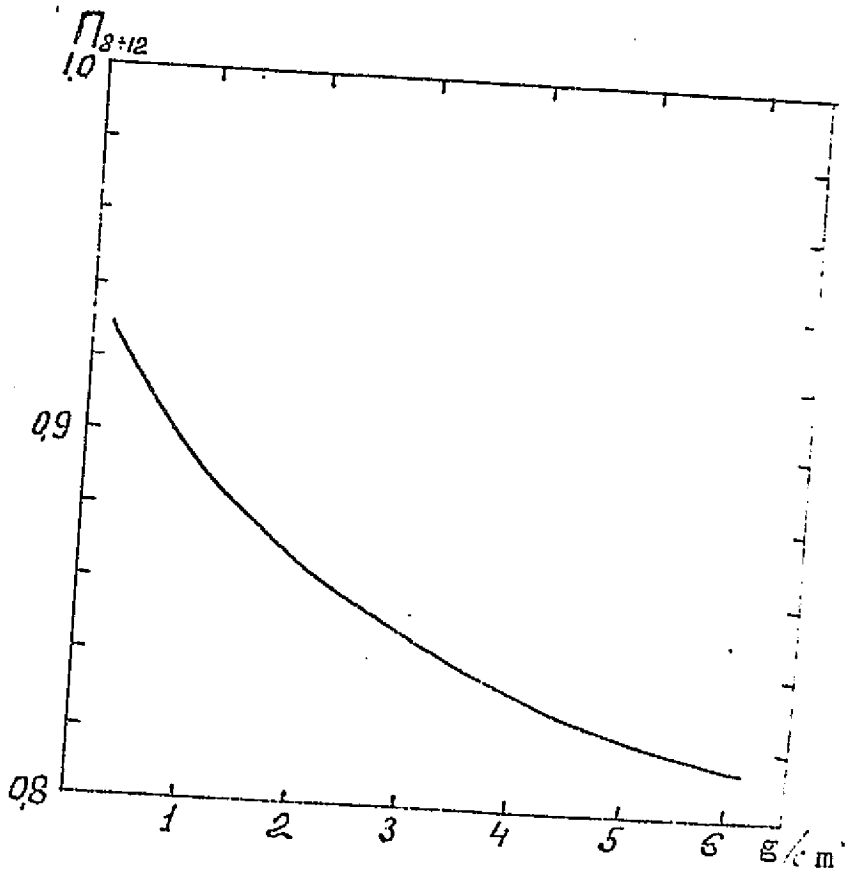

Fig. 49. [12] Dependence of the transmission function in the spectral interval 8÷12 μm on the moisture content of the atmosphere.

TABLE I

RADIATION COEFFICIENTS OF NATURAL FORMATIONS

No.	Formation \ Radiation coefficient/T K	ε [24]	ε [18a]	$\varepsilon_{8\div14}$ m [38]	$\varepsilon_{8\div12}$ m [12]	$\varepsilon_{9\div12}$ m [10]
I	2	3	4	5	6	7
I	Black earth		0,87/295			
2	Sandy loam, dry	0,92/293				0,954/-
3	Sandy loam, damp	0,95/293	0,95/295			0,968/-
4	Peat, dry					0,970/-
5	Peat, damp					0,983/-
6	Fine-grained sand, dry	0,90/293	0,89/295			0,949/-
7	Fine-grained sand, damp			0,928/-		0,962/-
8	Coarse-grained sand, dry			0,914/-		
9	Coarse-grained sand, damp			0,936/-		
I0	Sandstone, rough surface			0,935/-		
II	Gravel		0,91/295			
I2	Coarse gravel, 0.5 cm pieces			0,94÷0,96		
I3	Fine gravel, basaltic			0,952/-		
I4	Basalt				0,904/-	
I5	Basalt, rough surface			0,934/-		
I6	Granite				0,815/-	
I7	Granite, rough surface			0,898/-		
I8	Dolomite				0,829/-	
I9	Dolomite, rough surface			0,958/-		

TABLE I (con't)

I	2	3	4	5	6	7
20	Dunite				0,856/-	
2I	Dunite, rough surface				0,892/-	
22	Obsidian				0,862/-	
23	Obsidian, rough surface				0,837/-	
24	Quartz				0,7I2/-	
25	Feldspar				0,970/-	
26	Limestone		0,9I/295			
27	Yellow clay		0,85/295			
28	Sparse grass		0,84/295			
29	Sparse grass in sandy loam					0,975/-
30	Rye field		0,93/295			
3I	Green grass, thick		0,97/295	0,973/-		0,986/-
32	Coniferous needles		0,97/295			0,97I/-
33	Clean water	0,96/293			0,993/-	0,96 /-
34	Water covered with automobile oil				0,973/-	
35	Sea water		0,96/298			
36	Smooth ice	0,96/263				
37	Grainy ice	0,98/263			0,980/-	
38	Fresh fallen snow, dry	0,85/263	0,97÷0,99		0,996/270	0,986/-
39	Dirty snow					0,969/-
40	Snow, moist				0,997/273	
4I	Snow, melting				0,995/-	
42	Cloud				0,I5÷0,99	

REFERENCES

1. Afans'ev, N. F., "Statisticheskiy analyz aerofotoizobrazheniy" V. sb. Issledovanie opticheskikh svoystv prirodnykh ob'ektov i ikh aerofotograficheskogo izobrazheniya [Statistical Analysis of Aerial Photographs in coll. Investigations of the Optical Characteristics of Natural Objects and Aerial Photographs of Them]. Leningrad, Nauka [Science], 1970, pp. 114-123. /31

2. Bramson, M. A., "Infrakrasnoye izlucheniye nagretnykh tel" . [Infrared Studies of Heated Substances] Moscow, Nauka [Science], 1964.

3. Grigor'ev, M. A., Vinogradov, B. V., Cherpenko, A. P., "Infrakrasnaya aeros'emka i nazemnye issledovaniya termal'noy struktury landshafta sukhikh stepey." V. sb. Issledovanie prirodnoy sredy kosmicheskimi sredstvami [Infrared Aerial Survey and Terrestrial Investigations of the Thermal Structure of Dry Steppe Landscapes . in coll. Investigations of Natural Atmospheres by Cosmic Methods], Moscow, USSR Academy of Sciences, 1974, vol. 3.

4. Gayevskiy, V. L., Rabinovich, Yu. I., Reshetnikov, A. I., "Ob izmerenii temperatury vody Kaspiyskogo morya s pomosch'yu radiatsionnogo termometra" [On Measuring the Temperature of Water in the Caspian Sea with a Solar Thermometer], GGO [Main Geophysical Observatory], 1965, issue 170, pp. 202-206.

5. Glagolyev, Yu. A., Spravochnik po fizicheskim parametram atmosfery [Handbook of Physical Parameters of the Atmosphere], Leningrad, Gidrometeoizdat, 1970.

6. Zhvalev, V. F., Kondrat'ev, K. Ya., Ter-Markaryants, N. Ye., "O raschete spektral'nykh velichin ukhodyaschego izlucheniya i kontrastov mezhdu radiatsionnoy temperaturoy podstilayuschyey poverkhnosti i oblakov v svyazi s zadachyey obnaruzheniy oblachnosti s ISZ" [On Calculating Spectral Values of Emitted Radiation and Contrasts between the Radiation Temperature of the Underlying Surface and Clouds in Connection with Detection of Cloud Covers with an Artificial Earth Satellite], Leningrad, GGO [Main Geophysical Observatory], 1967, issue 203.

7. Zaytsyev, Yu. A., Mukhina, L. A., "Primeneniye tsvetnoy i spektral'noy aerofotos'emki v geologicheskikh tselyakh"[Taking Color and Spectral Aerial Photographs of Geological Objects], MGU [Moscow State University], 1966.

8. Zuyev, V. E., "Prozrachnost' atmosfery dlya vidimykh i infrakrasnykh luchey" [Transmittance of the Atmosphere for Visible and Infrared Rays], Moscow Sovetskoye radio, 1966.

9. "Issledovaniya prirodnoy sredy s pilotiruemykh orbital'nykh stantsiy" [Investigations of Natural Atmospheres with Manned Orbital Stations], Leningrad, Gidrometeoizdat, 1972.

10. Kondrat'ev, K. Ya., "Aktinometriya" [Actinometry], Leningrad, Gidrometeoizdat, 1965. /32

11. Kondrat'ev, K. Ya., Smotkiy, O. I., "Ob opredelenii peredatochnoy funktsii atmosfery pri spektrofotometrirovanii poverkhnosti planety iz kosmosa" [On Determining the Transmission Function of the Atmosphere During Spectrophotometry of the Planet's Surface from Space] Report USSR Academy of Sciencies, 1972, vol. 206, No. 5, pp. 1102-1105.

12. Kondrat'ev, K. Ya., Timofeev, Yu. M., "Termicheskoye zondirovaniye atmosfery so sputnikov" [Heat Sensing of the Atmosphere from Satellites], Leningrad, Gidrometeoizdat, 1970

13. Korzov, V.I., Krasil'schikov, L. B., "Nekotorye rezul'tati izmereniy spektral'nykh koeffitsientov yarkosti v oblast 0,7÷2.5 μm" [Some Results on Measurements of Spectral Brilliance Coefficients in the interval 0,7÷2.5 μm] Leningrad, GGO [Main Geophysical Observatory], 1966, issue 183, pp. 27-35.

14. Kriksunov, L. Z., Usol'tsev, I. F., "Infrakrasnye sistemy" [Infrared Systems] Moscow, Sovetskoye radio, 1968.

15. Krinov, E. L. "Spektral'naya otrazhatel'naya sposobnost' prirodnykh obrazovaniy" [The Spectral Reflective Powers of Natural Formations], Moscow, USSR Academy of Sciences, 1947.

16. Kuchko, A. S. "Aerofotografiya" [Aerial Photography] Moscow, Nedra, 1974.

17. Meleshko, K. E. "Izluchenie spektral'nykh koeffitsientov yarkosti prirodnykh ob'ektov v polevykh usloviyakh" V. sb. Issledovanie opticheskikh svoystv prirodnykh ob'ektov i ikh aerofotograficheskogo izobrazheniya [Studies of the Spectral Brilliance Coefficients of Natural Objects under Field Conditions in coll. Investigations of the Optical Properties of Natural Objects and Aerial Photographs of Them], Leningrad, Nauka [Science], 1970, pp. 16-34.

18. Meleshko, K. E., Kropov, P. A. "Vybor zon spektra dlya spektrometricheskoy aerofotos'emki lesnykh nasazhdeniy" V. sb. Doklady Komissii aeros'emki i fotografii, [Selection of

Spectral Zones for Spectrometric Aerial Surveys of Forest Vegetation in coll. Reports of the Committee on Aerial Surveys Photographs] Leningrad, Geografichkesogo obschestva USSR, 1969, issue 7, pp. 81-89.

18a. Pavlov, A. V. "Optiko-elektronnye pribory" [Optical-Electric Instruments], Moscow, Energiya, 1974.

19. "Radiatsionnye kharakteristiki atmosfery i zemnoy poverkhnosti" (pod red. K. Ya. Kondrat'ev) [Radiation Characteristics of the Atmosphere and Earth's Surface](ed. by K. Ya. Kondrat'ev), Leningrad, Gidrometeoizdat, 1969. /33

20. Sergeev, G. A., Yanutsh, D. A., "Statisticheskie metody issledovaniya prirodnykh ob'ektov" [Statistical Methods of Studying Natural Objects], Leningrad, Gidrometeoizdat, 1973.

21. Soul, Kh., "Elektronno-opticheskoye fotografirovanie" (per. s angl.) [Electronic-Optical Photography (trans. from Eng.)], Moscow, Voennoye MO USSR, 1972.

22. Feygel'son, E. M., Malkevich, M. C., et al. "Raschet yarkosti sveta v atmosfere pri anisotropic rasseyanii" [Calculation of Light Brilliance of the Atmosphere During Scattering] Institute of Atmospheric Physics of the USSR Academy of Sciences, Part I, 1958, No. 1, pp. 102; Part II, 1962, No. 3, pp. 1-223.

23. Fisher, V. A., "Sovremennoye sostoyanie tekhniki distantsionnogo zondirovaniya" [Contemporary Techniques in Remote Probing] Sluzhba geologicheskoy s'emki SShA [Geological Survey Service of the USA], trans. PP-37, IKI USSR Academy of Sciences, Moscow, 1974

24. Khadson, R., "Infrakrasnye sistemy" [Infrared Systems] (trans. from Eng.), Moscow, Mir, 1972.

25. Khalemskiy, E. N. "Spektral'noye raspredeleniye koeffitsienta yarkosti morya v vodakh s raznymi opticheskimi svoystvami" V. sb. Optika okeana i atmosfery [Spectral Distribution of Brilliance Coefficients in the Ocean for Water with Various Optical Characteristics. in coll. Optics of Oceans and Atmospheres], Leningrad, Nauka, pp. 187-192.

26. Chapurskiy, L. I. "Eksperimental'nye issledovaniya spektral'nykh yarkostnykh kharakteristik oblakov, atmosfery i podstilayuschey poverkhnosti v intervale dlin voln 0.3-2.5 μm." [Experimental Investigations of Spectral Brilliance Characteristics of Clouds, Atmospheres, and Underlying Surfaces in the wavelength interval 0.3-2.5 μm.] GGO [Main Geophysical Observatory], 1966, issue 196, pp. 110-119.

27. Shifrin, K. S. , Minin, I. N., "K teorii negorizontal'noy vidimosti" [Towards a Theory of Non-horizontal Visibility], GGO [Main Geophysical Observatory], Leningrad, 1957, issue 68, pp. 5-75.

28. Shifrin, K. C. , Shubova, G. L. "Dnevnoy khod prozrachnosti atmosfery" [The Diurnal Course of Atmospheric Transmittance], GGO [Main Geophysical Observatory], Leningrad, 1970, issue 235, pp. 175-185.

29. Shubova, G. L. "Godovoy khod vertikal'noy prozrachnosti atmosfery." [The Annual Course of Vertical Transmittance in the Atmosphere], GGO [Main Geophysical Observatory], Leningrad, 1966, issue 196, pp. 103-109.

30. Yakovlev, A. A. "O svyazi kovariatsiy i korrelyatsiy spektral'nykh in integral'nykh yarkostyey prirodnykh ob'ektov s kovariatsiyami logarifmov yarkostyey" [On the Connection between Covariations and Correlations of Spectral and Integral Brilliances of Natural Objects and Covariations in Brilliance Logarithms], Information from the USSR Academy of Sciences, series Fizika atmosfery i okeana, 1975, vol. II, No. 6, pp. 639-642.

31. Biehl, L. L., Silva, L. F. "A Multilevel Multispectral Date Set /34
Analysis in the Visible and Infrared Wavelength Region". Pros. of the IEEE, 1975, v. 63, n. 1, pp. 164-175.

32. Evans, Wm. E. "Marking ERTS Images with a Small Mirror Reflector" Photogrammetric Engineering, 1974, v. 40, n. 6, pp. 665-671.

33. Gausman, H. W."Leaf Reflectans of Near-Infrared" Photogrammetric Engineering, 1974, v. 40, n. 2, pp. 183-191.

34. Hovis, W. A. "Optimum Wavelength Intervals for Surface Temperature Radiometry" Applied Optics, 1966, v. 5, n. 5 pp. 815-821.

35. Hovis, W. A. , Blaine, L. R., Callahan, W. R. "Infrared Aircraft Spectra over Desert Terrain 8.5 mcm to 16 mcm" Applied Optics, 1968, v. 7, n. 6, pp. 1137-1140.

36. Hovis, W. A. , Callahan, W. R., "Infrared Reflectance Spectra of Igneous Rocks, Tuffs, and Red Sandstone from 0.5 to 22 mcm. " J. Opt. Soc. Am., 1966, v. 56, n. 5 pp. 639-644.

37. Le Gault, R. "Sources of Electromagnetic Radiation" AIAA Paper, 1970, n. 70-287.

38. Lorenz, D., "Temperature Measurements of Natural Surfaces Using Infrared Radiometers" Applied Optics, 1968, v. 7 n. 9, pp. 1705-1710.

39. Peacock, K., Withrington, R., "An Orbiting Multispectral Scanner for Overland and Oceanographic Applications" Proc. Seventh International Symposium on Remote Sensing of Environment, Ann Arbor, Michigan, 1971.

40. Van Lopic, J. R., Pressman, A. E., Ludlum, R. L. "Mapping Pollution with Infrared", Photogrammetric Engineering, 1968, v. 34, n. 6, pp. 561-564.

41. Vincent, R. K. "The Potential Role of Thermal Infrared Multispectral Scanners in Geological Remote Sensing" Proc. of the IEEE, 1975, v. 63, n.1, pp. 137-147. /35

42. Vizy, K. N. "Detecting and Monitoring Oil Slicks with Aerial Photos" Photogrammetric Engineering, 1974, v. 40, n. 6, pp. 697-708.

43. Watson, K. "Geologic Applications of Thermal Infrared Images. Proc. of the IEEE, 1975, v. 63, n.1, pp. 128-137.

44. Zaitzeff,E. M., Wilson, C. L., Ebert, D. H., "MSDS: an Experimental 24-channel Multispectral Scanner System", Bendix Technical Journal, 1970, summer/autumn.